arXiv:1612.04846v1 [math.NA] 14 Dec 2016

OPTIMAL SOLVERS FOR LINEAR SYSTEMS WITH FRACTIONAL POWERS OF SPARSE SPD MATRICES

STANISLAV HARIZANOV, RAYTCHO LAZAROV, PENCHO MARINOV, SVETOZAR MARGENOV, AND YAVOR VUTOV

Abstract. In this paper we consider efficient algorithms for solving the algebraic equation $\mathcal{A}^\alpha \mathbf{u} = \mathbf{f}$, $0 < \alpha < 1$, where $\mathcal{A}$ is a symmetric and positive definite matrix obtained form finite difference or finite element approximations of second order elliptic problems in $\mathbb{R}^d$, $d = 1, 2, 3$. The method is based on the best uniform rational approximation of the function $t^{\beta-\alpha}$ for $0 < t \leq 1$ and natural β, and the assumption that one has at hand an efficient method (e.g. multigrid, multilevel, or other fast algorithm) for solving equations like $(\mathcal{A} + c\mathcal{I})\mathbf{u} = \mathbf{f}$, $c \geq 0$. The provided numerical experiments on model problems with $\mathcal{A}$ obtained by finite element approximation of elliptic equations in one and three spacial dimensions confirm the efficiency of the proposed algorithms.

AMS classification: 65F50, 65F10, 65D15, 65N22

Key words: symmetric positive definite matrices, fractional powers of matrices, fast solvers of fractional power matrix equations

1. Introduction

Let $\mathcal{A} \in \mathbb{R}^{N\times N}$ be a symmetric and positive definite matrix (SPD) generated by a finite element or finite difference approximation of some self-adjoint elliptic problem. In this paper we shall discuss an efficient method for solving algebraic systems of linear equations involving fractional power $\mathcal{A}^\alpha$, $0 < \alpha < 1$. Namely, we are interested in efficient algorithms for solving the problem

$$\text{find } \mathbf{u} \in \mathbb{R}^N \text{ such that } \quad \mathcal{A}^\alpha \mathbf{u} = \mathbf{f} \quad \text{for given } \quad \mathbf{f} \in \mathbb{R}^N \text{ and an SPD matrix } \mathcal{A}. \tag{1}$$

The fractional power $\mathcal{A}^\alpha$, $0 < \alpha < 1$, of a symmetric positive definite matrix $\mathcal{A}$ is expressed by the spectral representation of $\mathbf{u}$ through the eigenvalues and eigenvectors $\{(\Lambda_i, \mathbf{\Psi}_i)\}_{i=1}^N$ of $\mathcal{A}$. We assume that the eigenvectors are l_2-orthonormal, i.e. $\mathbf{\Psi}_i^T \mathbf{\Psi}_j = \delta_{ij}$ and $\Lambda_1 \leq \Lambda_2 \leq \dots \Lambda_N$. We consider the case when the matrix $\mathcal{A}$ is ill-conditioned, namely, the spectral condition number $\mathrm{k}(\mathcal{A}) = \Lambda_N/\Lambda_1$ is large. Then $A = WDW^T$ and $\mathcal{A}^\alpha = WD^\alpha W^T$, where the $N \times N$ matrices W and D are defined as $W = [\mathbf{\Psi}_1^T, \mathbf{\Psi}_2^T, ..., \mathbf{\Psi}_N^T]$ and $D = diag(\Lambda_1, \dots, \Lambda_N)$. Then $\mathcal{A}^{-\alpha} = WD^{-\alpha}W^T$ and the solution of $\mathcal{A}^\alpha \mathbf{u} = \mathbf{f}$ can be expressed as

$$\mathbf{u} = \mathcal{A}^{-\alpha}\mathbf{f} = WD^{-\alpha}W^T\mathbf{f}. \tag{2}$$

Obviously, we have the following standard equality for any $\beta \in \mathbb{R}$:

$$\|\mathbf{u}\|_{\mathcal{A}^{\beta+\alpha}} = \|\mathbf{f}\|_{\mathcal{A}^{\beta-\alpha}} \quad \text{with} \quad \|\mathbf{u}\|^2_{\mathcal{A}^\gamma} = \mathbf{u}^T\mathcal{A}^\gamma\mathbf{u}, \quad \gamma \in \mathbb{R}.$$

This formula could be used in practical computations if the eigenvectors and eigenvalues are explicitly known and the matrix vector multiplication with W is equivalent to a Fast Fourier Transform (FFT), e.g. $\mathcal{A}$ is a circulant matrix. In such cases the computational complexity is almost linear, $O(N \log N)$. However, this limits the applications to problems with constant coefficients in simple domains and, e.g., to the lowest order finite element approximations. More general is the approach using an approximation of $\mathcal{A}$ with H-matrices combined with Kronecker tensor-product approximation, see, [9]. This allows computations with almost linear complexity of the inverse of fractional power of a discrete elliptic operator in a hypercube $(0, 1)^d \in \mathbb{R}^d$, for more details, see [9].

Date: December 16, 2016.

This work is related to the more difficult problem of stable computations of the matrix square root and related functions, e.g. [7, 13, 15], where the stabilization of Newton method is achieved by using suitable Padé iteration. However, in this paper we do not deal with evaluation of $\mathcal{A}^\alpha$, instead we propose an efficient method for solving the algebraic system $\mathcal{A}^\alpha \mathbf{u} = \mathbf{f}$, where $\mathcal{A}$ is an SPD matrix generated by finite element approximation of second order elliptic operators. Our research is also connected with the work done in [14], where numerical approximation of a fractional-in-space diffusion equation with non-homogeneous boundary conditions is considered. In [14], the proposed solver of the arising algebraic system relies on Lanczos method. First, the adaptively preconditioned thick restart Lanczos procedure is applied to a system with $\mathcal{A}$. The gathered spectral information is then used to solve the system with $\mathcal{A}^\alpha$. Essentially, this approach and the method proposed and used in [11] rely on polynomial approximation of $t^{-\alpha}$, and the efficiency of the methods depends on the condition number of $\mathcal{A}$.

Our work is motivated by the recent development in the fractional calculus and its numerous applications to Hamiltonian chaos, anomalous transport, and super-diffusion, [24], anomalous diffusion in complex systems such as turbulent plasma, convective rolls, and zonal flow system, [1], long-range interaction in elastic deformations, [21], nonlocal electromagnetic fluid flows, [18], image processing, [10], nonlocal evolution equations arising in materials science, [2]. Often, these involve fractional derivatives of Riemann-Liouville or Caputo type or in the symmetric case, the Riesz derivative. A recent excellent discussion about various anomalous diffusion models, their properties and applicability to chemistry and engineering one can find in [19]. These applications lead to various types of fractional order partial differential equations that involve in general non-symmetric elliptic operators see, e.g. [16]. An important subclass of such problems are the fractional powers of self-adjoint elliptic operators, which are nonlocal but self adjoint.

We consider the following model problem in a weak form: find $u \in V$ such that

$$a(u,v) := \int_\Omega \left(\mathbf{a}(x)\nabla u(x)\cdot\nabla v(x) + q(x)\right) dx = \int_\Omega f(x)v(x)dx,\ \forall v \in V, \tag{3}$$

where

$$V := \{v \in H^1(\Omega) :\ v(x) = 0 \text{ on } \Gamma_D\},$$

$\Gamma = \partial\Omega$, and $\Gamma = \bar{\Gamma}_D \cup \bar{\Gamma}_N$. We assume that Γ_D has positive measure, $q(x) \geq 0$ in Ω, and $\mathbf{a}(x)$ is an SPD $d \times d$ matrix, uniformly bounded in Ω, i.e.,

$$c\|y\|^2 \leq y^T \mathbf{a}(x)\, y \leq C\|y\|^2 \quad \forall y \in \mathbb{R}^d, \forall x \in \Omega, \tag{4}$$

for some positive constants c and C. Also Ω is a polygonal domain in $\mathbb{R}^d$, $d = 1, 2, 3$, and $f(x)$ is a given Lebesgue integrable function on Ω that belongs to the space $L_2(\Omega)$. Further, the case when $\mathbf{a}(x)$ does not depend on x is referred to as problem in homogeneous media, while the general case models processes in non homogeneous media. The bilinear form $a(\cdot,\cdot)$ defines a linear operator $\mathcal{L} : V \to V^*$ with V^* being the dual of V. Namely, for all $u, v \in V$ $a(u,v) := \langle \mathcal{L}u, v\rangle$, where $\langle\cdot,\cdot\rangle$ is the pairing between V and V^*.

One possible way to introduce $\mathcal{L}^\alpha$ is through its spectral decomposition, i.e.

$$\mathcal{L}^\alpha u(x) = \sum_{i=1}^{\infty} \lambda_i^\alpha c_i \psi_i(x), \quad \text{where} \quad u(x) = \sum_{i=1}^{\infty} c_i \psi_i(x). \tag{5}$$

Here $\{\psi_i(x)\}_{i=1}^\infty$ are the eigenfunctions of $\mathcal{L}$, orthonormal in L_2-inner product and $\{\lambda_i\}_{i=1}^\infty$ are the corresponding positive real eigenvalues.

This definition is general, but quite different from the definition of the fractional powers of elliptic operators with homogeneous Dirichlet data defined through Ritz potentials, see, e.g. [3]. Such definition generalizes the concept of equally weighted left and right Riemann-Liouville fractional derivative defined in one space dimension to the multidimensional case. There is ongoing research about the relations of these two different definitions and their possible applications to problems in science and engineering, see, e.g. [2].

Although the approximation results in this paper are more general, let us assume that the SPD matrix $\mathcal{A}$ is produced by finite element approximation of the operator equation $\mathcal{L}u = f$.

Then the algebraic equation (1) is an approximation of the problem (3). Error analysis of such approximation can be done by using the methods developed in [3]. However, this is outside the scope of this paper and is left for future study.

Finite element approximations of $\mathcal{L}^\alpha u = f$, where $\mathcal{L} = -\Delta$ with homogeneous Dirichlet data and the fractional power is defined through Ritz potentials are considered in [3]. The developed algorithm is based on an integral representation of $u(x) = \mathcal{L}^{-\alpha} f(x)$ and the finite element approximation $\mathcal{L}_h$ of the elliptic operator $\mathcal{L}$ (in our terminology $\mathcal{L}_h = \mathcal{A}$). Among others, the authors propose an exponentially convergent quadrature scheme. The approximate solution only involves evaluations of $(I + t_i\mathcal{A})^{-1} f$ where $t_i \in (0, \infty)$ is related to the quadrature node. The method has optimal computational complexity, assuming that an optimal solver (e.g., multigrid, AMG, AMLI) is used to solve the arising auxiliary problems, namely, inverting the matrices $I + t_i\mathcal{A}$.

In [22] the algebraic problem arising in approximation of fractional power of the second-order elliptic operator is solved numerically using an auxiliary Cauchy problem for a pseudo-parabolic equation. The computational algorithm is implemented as two-level time-stepping scheme using the elliptic operator instead of its fractional power. Numerical experiments show the efficiency of the proposed method in the case of smooth f.

An alternative approach to the fractional diffusion problems is presented in [4]. To localize the nonlocal operator, the fractional power of Laplacian in Ω is represented as a Dirichlet-to-Neumann operator via an extension to a problem on the semi-infinite cylinder $\Omega \times (0, \infty)$. The proposed multilevel method is based on the Xu-Zikatanov identity [23]. The numerical tests for $\Omega = (0, 1)$ and $\Omega = (0, 1)^2$ confirm the theoretical estimates of almost optimal complexity.

There are various other problems leading to systems with fractional power of sparse symmetric and positive definite matrices. For an illustration we give the following examples. Consider a non-overlapping domain decomposition (DD) for the model Laplacian problem on a regular mesh with an interface along a single mesh line. The elimination of all degrees of freedom from the interior of the two subdomains reduces the solution to a system of equations on the interface, or the Schur complement system. The matrix of this system is spectrally equivalent to $\mathcal{A}^{1/2}$, where $\mathcal{A} = tridiag(-1, 2, -1)$, see, e.g. [20]. When in the preconditioned conjugate gradient (PCG) method FFT is used to solve the system with $\mathcal{A}^{1/2}$, then the DD preconditioner has almost optimal complexity. In [11] the best uniform polynomial approximation of $t^{-1/2}$, $t \in [\Lambda_1, 1]$, Λ_1 well separated from 0, is used to construct an optimal solver for the equation (1) with $\alpha = 0.5$. Such problems arise in the volume constrained 2-phase segmentation where $\mathcal{A}$ is an SPD matrix and belongs to a class of particular weighted graph Laplacian. The results of this paper have potential for substantial generalization and improvements regarding above two examples.

The paper is organized as follows. In Section 2 we introduce the mathematical problem and present the idea of the proposed algorithm. First, we argue that instead of the system $\mathcal{A}^\alpha \mathbf{u} = \mathbf{f}$ one can solve the equivalent system $\mathcal{A}^{\alpha-\beta}\mathbf{u} = \mathcal{A}^{-\beta}\mathbf{f}$ with $\beta \geq 1$ an integer. Then the idea is to approximately evaluate $\mathcal{A}^{\beta-\alpha}\mathbf{f}$ using a set of equations involving inversion of $\mathcal{A} - d_j I$, $d_j \leq 0$ for $j = 0, 1, \ldots, k$, see representation (21). The integer parameter $k \geq 1$ is the number of partial fractions of the best uniform rational approximation $r_\alpha^\beta(t)$ of $t^{\beta-\alpha}$ on the interval $(0, 1]$. The most general form of this method leads to (13). In Subsection 2.2 we discuss the way $r_\alpha^\beta(t)$ is obtained, its approximation properties and some relevant practical questions regarding the implementation. It is quite remarkable that in the number of practical cases we consider the denominator of the best rational approximation $r_\alpha^\beta(t)$ has only real roots and consequently the partial fraction representation has a very simple form, namely, it reduces to equation (21). Finally, in Section 4 we present a number of numerical experiments that illustrate the efficiency of the proposed algorithm.

2. Problem formulation

2.1. **The idea of the method.** The goal of this study is to present a new robust solver of optimal complexity for solving the system (1) for a large class of sparse SPD matrices assuming that such a solver is available for $\alpha = 1$. This assumption holds in a very general setting, when $\mathcal{A}$

is generated by finite element or finite difference approximation of second order elliptic operators. Such matrices are used in the numerical tests presented in Section 4. Note that $\mathcal{A}^\alpha$ is dense and in general not known. This means in particular that the standard iterative solution methods are not applicable since even in the case when $\mathcal{A}^\alpha\mathbf{u}$ is computable just one such computation requires $O(N^2)$ arithmetic operations.

We assume that we have performed a suitable rescaling of the matrix $\mathcal{A}$ so that its spectrum is in the interval $(0,1]$, i.e. $0<\Lambda_1\le\cdots\le\Lambda_N\le 1$. Here we present a new method based on the approximation of the fractional power $\mathcal{A}^{-\alpha}$ by a rational function of $\mathcal{A}$. We begin with a simple observation that is a basis of our approach.

Theorem 2.1. *Assume that for β positive integer number and $\alpha\le\beta$ the univariate function $r_\alpha^\beta(t)$ is analytic on $(0,1]$ and for a given constant $\varepsilon>0$ satisfies*

$$|r_\alpha^\beta(t)-t^{\beta-\alpha}|\le\varepsilon,\qquad \forall t\in(0,1]. \tag{6}$$

Then, for any $\gamma\in\mathbb{R}$ and $\mathbf{F}\in\mathbb{R}^N$ we have

$$\|r_\alpha^\beta(\mathcal{A})\mathbf{F}-\mathcal{A}^{\beta-\alpha}\mathbf{F}\|_{\mathcal{A}^\gamma}\le\varepsilon\|\mathbf{F}\|_{\mathcal{A}^\gamma}. \tag{7}$$

Proof. Consider the spectral decomposition of $\mathbf{F}$ with respect to the eigenfunctions of $\mathcal{A}$, namely, $\mathbf{F}=\sum_{i=1}^N F_i\mathbf{\Psi}_i$ so that, $\|\mathbf{F}\|^2_{\mathcal{A}^\gamma}=\sum_{i=1}^N\Lambda_i^\gamma F_i^2$, for any $\gamma\in\mathbb{R}$. Since r_α^β is analytic in $(0,1]$, it has convergent Maclaurin expansion there and therefore $r_\alpha^\beta(\mathcal{A})\mathbf{\Psi}_i=r_\alpha^\beta(\Lambda_i)\mathbf{\Psi}_i$, $i=1,\dots,N$. Using the orthonormal property of the eigenvectors $\mathbf{\Psi}_i^T\mathbf{\Psi}_j:=\langle\mathbf{\Psi}_i,\mathbf{\Psi}_j\rangle=\delta_{ij}$ we get easily

$$\begin{aligned}\|r_\alpha^\beta(\mathcal{A})\mathbf{F}-\mathcal{A}^{\beta-\alpha}\mathbf{F}\|^2_{\mathcal{A}^\gamma}&=\left\langle\sum_{i=1}^N(\mathcal{A}^\gamma(r_\alpha^\beta(\mathcal{A})-\mathcal{A}^{\beta-\alpha})F_i\mathbf{\Psi}_i,\sum_{i=1}^N(r_\alpha^\beta(\mathcal{A})-\mathcal{A}^{\beta-\alpha})F_i\mathbf{\Psi}_i\right\rangle\\&=\sum_{i=1}^N F_i^2\Lambda_i^\gamma\left(r_\alpha^\beta(\Lambda_i)-\Lambda_i^{\beta-\alpha}\right)^2\le\max_{t\in[0,1]}|r_\alpha^\beta(t)-t^{\beta-\alpha}|^2\sum_{i=1}^N\Lambda_i^\gamma F_i^2\le\varepsilon^2\|\mathbf{F}\|^2_{\mathcal{A}^\gamma}.\end{aligned}$$

The proof is completed. □

Instead of the original equation $\mathcal{A}^\alpha\mathbf{u}=\mathbf{f}$ we consider the equivalently transformed equation $\mathcal{A}^{\alpha-\beta}\mathbf{u}=\mathcal{A}^{-\beta}\mathbf{f}:=\mathbf{F}$ with a small positive integer β, e.g., $\beta=1$ or $\beta=2$, and a solution $\mathbf{u}=\mathcal{A}^{-\alpha}\mathbf{f}=\mathcal{A}^{\beta-\alpha}\mathbf{F}$. Then $\mathbf{u}_r=r_\alpha^\beta(\mathcal{A})\mathcal{A}^{-\beta}\mathbf{f}$ is an approximation of $\mathbf{u}$ and the estimate (7) can be rewritten as

$$\|\mathbf{u}_r-\mathbf{u}\|_{\mathcal{A}^\gamma}=\|r_\alpha^\beta(\mathcal{A})\mathbf{F}-\mathcal{A}^{\beta-\alpha}\mathbf{F}\|_{\mathcal{A}^\gamma}\le\varepsilon\|\mathbf{F}\|_{\mathcal{A}^\gamma}.$$

Now taking in (7) $\gamma=1$ we get the following estimate for the difference $\mathbf{u}_r-\mathbf{u}$:

$$\|\mathbf{u}_r-\mathbf{u}\|_{\mathcal{A}^\gamma}=\|r_\alpha^\beta(\mathcal{A})\mathcal{A}^{-\beta}\mathbf{f}-\mathcal{A}^{-\alpha}\mathbf{f}\|_{\mathcal{A}^1}\le\varepsilon\|\mathbf{f}\|_{\mathcal{A}^{1-2\beta}}. \tag{8}$$

In particular, for the cases we consider, $\beta=1$ and $\beta=2$, we get correspondingly

$$\|r_\alpha^1(\mathcal{A})\mathcal{A}^{-1}\mathbf{f}-\mathcal{A}^{-\alpha}\mathbf{f}\|_{\mathcal{A}}\le\varepsilon\|\mathbf{f}\|_{\mathcal{A}^{-1}}\quad\text{and}\quad\|r_\alpha^2(\mathcal{A})\mathcal{A}^{-2}\mathbf{f}-\mathcal{A}^{-\alpha}\mathbf{f}\|_{\mathcal{A}}\le\varepsilon\|\mathbf{f}\|_{\mathcal{A}^{-3}}. \tag{9}$$

Similarly, for $\gamma=\alpha$ we get

$$\|r_\alpha^\beta(\mathcal{A})\mathcal{A}^{-\beta}\mathbf{f}-\mathcal{A}^{-\alpha}\mathbf{f}\|_{\mathcal{A}^\alpha}\le\varepsilon\|\mathbf{f}\|_{\mathcal{A}^{\alpha-2\beta}}, \tag{10}$$

and $\beta=1$ and $\beta=2$

$$\|r_\alpha^1(\mathcal{A})\mathcal{A}^{-1}\mathbf{f}-\mathcal{A}^{-\alpha}\mathbf{f}\|_{\mathcal{A}^\alpha}\le\varepsilon\|\mathbf{f}\|_{\mathcal{A}^{\alpha-2}}\quad\text{and}\quad\|r_\alpha^2(\mathcal{A})\mathcal{A}^{-2}\mathbf{f}-\mathcal{A}^{-\alpha}\mathbf{f}\|_{\mathcal{A}^\alpha}\le\varepsilon\|\mathbf{f}\|_{\mathcal{A}^{\alpha-4}}. \tag{11}$$

Therefore, $\mathbf{u}_r=r_\alpha^\beta(\mathcal{A})\mathcal{A}^{-\beta}\mathbf{f}$ is an approximation of the exact solution with relative error less than or equal to ε. The error estimator ε doesn't dependent on the matrix $\mathcal{A}$, i.e., it is robust. Similar computational techniques as those in Theorerm 2.1 were used before, for example in [6].

Based on this observation in this paper we present a robust method for solving $\mathcal{A}^{\alpha-\beta}\mathbf{u}=\mathbf{F}$ with optimal complexity by using best uniform (m,k)-rational approximation of $t^{\beta-\alpha}$, $\beta=1,2$,

for $t \in (0,1]$. The idea of the method is to apply the partial fraction decomposition of $t^{-\beta} r_\alpha^\beta(t)$

$$t^{-\beta} r_\alpha^\beta(t) = \sum_{j=0}^{m-k-\beta} b_j\, t^j + \sum_{j=1}^{\beta} \frac{c_{0,j}}{t^j} + \sum_{j=1}^{p_1} \frac{c_j}{t-d_j} + \sum_{j=1}^{p_2} \frac{B_j t + C_j}{(t-F_j)^2 + D_j^2} \tag{12}$$

where $k = p_1 + 2\,p_2$, so that the approximate solution $\mathbf{u}_\beta = \mathcal{A}^{-\beta} r_\alpha^\beta(\mathcal{A})\mathbf{f}$ can be computed as

$$\begin{aligned} \mathcal{A}^{-\beta} r_\alpha^\beta(\mathcal{A})\mathbf{f} = \sum_{i=0}^{m-k-\beta} b_i \mathcal{A}^i \mathbf{f} + \sum_{i=1}^{\beta} c_{0,i} \mathcal{A}^{-i}\mathbf{f} + \sum_{i=1}^{p_1} c_i (\mathcal{A} - d_i I)^{-1}\mathbf{f} \\ + \sum_{i=1}^{p_2} (B_i \mathcal{A} + C_i I)((\mathcal{A} - F_i I)^2 + D_i^2 I)^{-1}\mathbf{f}. \end{aligned} \tag{13}$$

This shows that to find $\mathbf{u}_r = r_\alpha^\beta(\mathcal{A})\mathcal{A}^{-\beta}\mathbf{f}$ we need to solve systems with $\mathcal{A}$, with the SPD matrices $\mathcal{A} - d_i I$ for $i = 1, \dots p_1$ and with $(\mathcal{A} - F_i I)^2 + D_i^2 I$, for $i = 1, \dots, p_2$. We show that for a good accuracy in the approximation (6) we get small number of factors, namely k is small.

Remark 2.2. *Our numerical tests show that often we achieve accuracy of $\epsilon = 10^{-5}$ or higher in (8) with $p_1 = 5$ or $p_1 = 6$ and $p_2 = 0$. Note that for $p_2 = 0$ the corresponding algorithm for solving the algebraic system is in general simpler and more efficient.*

2.2. **Best uniform rational approximation.** We consider $r_\alpha^\beta(t)$ within the class of rational functions

$$\mathcal{R}(m,k) := \{r_\alpha^\beta(t) = P_m/Q_k \,:\, P_m \in \mathcal{P}_m, Q_k \in \mathcal{P}_k\},$$

where $\mathcal{P}_k$ is the set of all polynomials of degree k.

For a given univariate function $F(t)$ the minimizer $r^*(t) = \frac{P_m^*(t)}{Q_k^*(t)} \in \mathcal{R}(m,k)$ of the problem

$$\min_{r \in \mathcal{R}(m,k)} \max_{t\in[0,1]} |F(t) - r(t)| = \max_{t\in[0,1]} |F(t) - r^*(t)| \tag{14}$$

is called Best Uniform Rational Approximation (BURA). In the particular case $F(t) = t^{\beta-\alpha}$ the minimizer $r_\alpha^\beta(t) = \frac{P_m^*(t)}{Q_k^*(t)}$ is called further *β-Best Uniform Rational Approximation* (β-BURA) and its error is denoted by

$$E_\alpha(m,k;\beta) := \max_{t\in[0,1]} \left| t^{\beta-\alpha} - \frac{P_m^*(t)}{Q_k^*(t)} \right|.$$

Then we have the following error bound for any $\gamma > 0$

$$\begin{aligned} \|\mathbf{u}_r - \mathbf{u}\|_{\mathcal{A}^\gamma}^2 &= \left\| \mathcal{A}^{-\beta} \left(r_\alpha^\beta(\mathcal{A})\mathbf{f} - \mathcal{A}^{\beta-\alpha}\mathbf{f} \right) \right\|_{\mathcal{A}^\gamma}^2 = \|r_\alpha^\beta(\mathcal{A})\mathbf{f} - \mathcal{A}^{\beta-\alpha}\mathbf{f}\|_{\mathcal{A}^{\gamma-2\beta}}^2 \\ &\le \max_{0\le t\le 1} |r_\alpha^\beta(t) - t^{\beta-\alpha}|^2 \|\mathbf{f}\|_{\mathcal{A}^{\gamma-2\beta}}^2 = E_\alpha^2(m,k;\beta)\|\mathbf{f}\|_{\mathcal{A}^{\gamma-2\beta}}^2. \end{aligned} \tag{15}$$

In particular, for $\beta = 1$, we get

$$\|\mathbf{u}_r - \mathbf{u}\|_{\mathcal{A}^\alpha} \le E_\alpha(m,k;1)\|\mathbf{f}\|_{\mathcal{A}^{\alpha-2}}, \quad \gamma = \alpha \quad \text{and} \quad \|\mathbf{u}_r - \mathbf{u}\|_{\mathcal{A}} \le E_\alpha(m,k;1)\|\mathbf{f}\|_{\mathcal{A}^{-1}}, \quad \gamma = 1$$

and similarly for $\beta = 2$

$$\|\mathbf{u}_r - \mathbf{u}\|_{\mathcal{A}^\alpha} \le E_\alpha(m,k;2)\|\mathbf{f}\|_{\mathcal{A}^{\alpha-4}}, \quad \gamma = \alpha \quad \text{and} \quad \|\mathbf{u}_r - \mathbf{u}\|_{\mathcal{A}} \le E_\alpha(m,k;2)\|\mathbf{f}\|_{\mathcal{A}^{-3}} \quad \gamma = 1.$$

We always consider triples (m,k,β) for which $m < k+\beta$. One reason for such a parameter constraint comes from the fact that $t^{-\beta} r_\alpha^\beta$ has a leading term of degree $t^{m-k-\beta}$, while it approximates the power function $t^{-\alpha}$, $\alpha > 0$. Another reason is the numerical simplification of (12), where the index set for the first sum becomes empty. In all our numerical examples the denominator of r_α^β

has no complex roots, thus we concentrate on the case $p_2 = 0$ from now on. Then β-BURA can be rewritten in the following way:

$$\frac{1}{t^\beta}\,\frac{P_m^*(t)}{Q_k^*(t)} = \frac{\sum\limits_{j=0}^{m} p_j\ t^j}{t^\beta\left(\sum\limits_{j=0}^{k} q_j\ t^j\right)} = \sum_{j=1}^{\beta}\frac{c_{0,j}}{t^j} + \sum_{j=1}^{k}\frac{c_j}{t-d_j}. \tag{16}$$

The first representation in (16) is the best approximation written as a standard rational function, while the second one is its partial fraction decomposition (12), the way this approximation is used in the implementation of the method.

Let

$$\frac{P_m^*(t)}{Q_k^*(t)} = \sum_{j=0}^{\beta-1} b_j^* t^j + \sum_{j=1}^{k}\frac{c_j^*}{t-d_j}.$$

We have used that $\beta > m-k$ and we set the extra coefficients $\{b_j^*\}_{m-k+1}^{\beta-1}$ to zero whenever $m-k<\beta-1$. Then, straightforward computations give rise to

$$\frac{1}{t^\beta}\,\frac{P_m^*(t)}{Q_k^*(t)} = \sum_{j=1}^{\beta}\frac{b_{\beta-j}^*}{t^j} + \sum_{j=1}^{k}\left(\frac{c_j^*/d_j^\beta}{t-d_j} - \sum_{i=1}^{\beta}\frac{c_j^*/d_j^{\beta-i+1}}{t^i}\right). \tag{17}$$

Comparing the coefficients in front of the corresponding terms in (16) and (17), we derive

$$c_{0,j} = b_{\beta-j}^* - \sum_{i=1}^{k} c_i^*/d_i^{\beta-j+1}, \qquad c_j = c_j^*/d_j^\beta. \tag{18}$$

Various useful identities follow from (18). We want to highlight a couple of them. Due to the Chebyshev's equioscillation theorem

$$c_{0,\beta} = b_0^* - \sum_{i=1}^{k} c_j^*/d_j = \frac{P_m^*(0)}{Q_k^*(0)} = \frac{p_0}{q_0} = \pm E_\alpha(m,k;\beta). \tag{19}$$

The second one is

$$c_{0,1} + \sum_{i=1}^{k} c_i = b_{\beta-1}^* = \begin{cases} p_m/q_k, & m-k=\beta-1; \\ 0, & m-k<\beta-1. \end{cases} \tag{20}$$

In the most interesting for us case, $\beta = 1$, we have just one coefficient $c_{0,1}$ which will be for convenience denoted by c_0. In this case introducing also $d_0 = 0$ the above representation is simplified to

$$\frac{1}{t}\,\frac{P_m^*(t)}{Q_k^*(t)} = \sum_{j=0}^{k}\frac{c_j}{t-d_j}. \tag{21}$$

These notations are used in the tables below.

Now we present some examples of β-BURA r_α^β within the class $\mathcal{R}(m,m)$ for $\alpha = 0.75, 0.5, 0.25$. In Table 1 we give the corresponding errors $E_\alpha(m,m;\beta)$ for some selected combinations of $m \in \{5,6,7\}$ and $\beta \in \{1,2,3\}$. In Tables 2 - 4 we show the computed coefficients (21) for $\alpha =$ 0.75, 0.5, 0.25, $\beta = 1$. When $\beta = 1$ and $m = k$, the identities (19) and (20) simplify to $c_0 = p_0/q_0 = E_\alpha(m,m;1)$ and $\sum_i c_i = p_m/q_m = p_m$. One can directly check that the numerical results in Tables 1 - 4 perfectly align with both of them. The data from Table 3 can be written also in terms of partial fractions

$$\begin{aligned}\frac{r_{0.5}^1(t)}{t} = \frac{P_m^*(t)}{t\,Q_k^*(t)} = {} & \frac{0.0002689}{t} + \frac{0.0055848}{t+0.0000122} + \frac{0.0272036}{t+0.0006621} \\ & + \frac{0.0965749}{t+0.0127955} + \frac{0.3202068}{t+0.1626313} + \frac{2.5105702}{t+3.2129222}.\end{aligned} \tag{22}$$

TABLE 1. Errors $E_\alpha(m,m;\beta)$ of BURA $P_m^*(t)/Q_m^*(t)$ of $t^{\beta-\alpha}$ on$[0,1]$

α	$E_\alpha(5,5;1)$	$E_\alpha(6,6;1)$	$E_\alpha(7,7;1)$	$E_\alpha(5,5;2)$	$E_\alpha(5,5;3)$
0.75	2.7162E-3	1.4312E-3	7.8966E-4	1.9015E-6	6.8813E-8
0.50	2.6896E-4	1.0747E-4	4.6037E-5	9.5789E-7	5.5837E-8
0.25	2.8676E-5	9.2522E-6	3.2566E-6	2.8067E-7	2.4665E-8

TABLE 2. The coefficients in (21) of BURA $P_5^*(t)/Q_5^*(t)$ of $t^{1-\alpha}$ on $[0,1]$, $\alpha = 0.75$

j	p_j	q_j	c_j	d_j
0	2.14466E-20	7.89576E-18	2.71622E-03	0.00000E+00
1	6.01477E-12	2.32380E-10	2.30450E-02	-3.40780E-08
2	1.81174E-06	2.00608E-05	6.32822E-02	-1.17193E-05
3	5.93157E-03	2.47161E-02	1.45623E-01	-8.24386E-04
4	4.91195E-01	8.78753E-01	3.05797E-01	-2.82243E-02
5	1.40119E+00	1.00000E+00	8.60727E-01	-8.49692E-01

TABLE 3. The coefficients in (21) of BURA $P_5^*(t)/Q_5^*(t)$ of $t^{1-\alpha}$ on $[0,1]$, $\alpha = 0.5$

j	p_j	q_j	c_j	d_j
0	1.45636E-14	5.41485E-11	2.68957E-04	0.00000E+00
1	2.87192E-08	4.51317E-06	5.58483E-03	-1.22320E-05
2	2.69846E-04	7.06745E-03	2.72036E-02	-6.62106E-04
3	8.87796E-02	5.67999E-01	9.65749E-02	-1.27955E-02
4	1.91330E+00	3.38902E+00	3.20207E-01	-1.62631E-01
5	2.96041E+00	1.00000E+00	2.51057E+00	-3.21292E+00

TABLE 4. The coefficients in (21) of BURA $P_5^*(t)/Q_5^*(t)$ of $t^{1-\alpha}$ on $[0,1]$, $\alpha = 0.25$

j	p_j	q_j	c_j	d_j
0	3.45490E-12	1.20483E-07	2.86755E-05	0.00000E+00
1	1.58841E-06	7.90871E-04	1.27509E-03	-1.59055E-04
2	4.13469E-03	2.10628E-01	9.58752E-03	-3.96701E-03
3	5.71109E-01	4.81422E+00	4.86842E-02	-4.47241E-02
4	7.40426E+00	1.11966E+01	2.55382E-01	-3.97136E-01
5	9.24225E+00	1.00000E+00	8.92729E+00	-1.07506E+01

Based on these particular results we can make the following observations:

(1) Tables 2 - 4 show that the approximation of the action of $\mathcal{A}^{-\alpha}$ via the application of the operator $\mathcal{A}^{-1}r_\alpha^1(\mathcal{A})$ involves solving six systems of linear equations with SPD matrices; we have assumed that each evaluation $\mathcal{A}^{-1}$ can be computed approximately by PCG method with optimal complexity.

(2) Summing these six solutions should be stable process since the coefficients in the sum of fractions (22) are small and positive and there should not be any loss of accuracy (or stability) that might come from subtracting large numbers.

(3) From Table 1 we see that we reduce the error in the approximation while increasing β from 1 to 3. However, this comes at a cost. For example the relative errors for $\beta = 1$ and $\beta = 2$ are given by (9). Obviously, the errors are measured in two different ways and if we want to make reasonable comparison we should replace $\mathcal{A}^{-3}$-norm in the second term by $\mathcal{A}^{-1}$-norm and then the condition number of $\mathcal{A}$ will appear in the estimate for that term, for more discussion, see Subsection 3.2.

3. Approximation of $t^{-\alpha}$ in the class of rational functions

3.1. **Theoretical background and numerical methods.** Let $r_\alpha^\beta(t) = \frac{P_m^*(t)}{Q_k^*(t)}$ be the β-BURA of $t^{\beta-\alpha}$ for $t \in [0,1]$. For given k and m, the rational function has the following representation:

$$\frac{P_m^*(t)}{Q_k^*(t)} = \frac{\sum\limits_{j=0}^{m} p_j t^j}{\sum\limits_{j=0}^{k} q_j t^j} = \frac{\sum\limits_{j=0}^{m} \bar{p}_j T_j(2t-1)}{\sum\limits_{j=0}^{k} \bar{q}_j T_j(2t-1)} = \frac{\bar{P}_m^*(s)}{\bar{Q}_k^*(s)}, \tag{23}$$

where $T_0(s) = 1,\ T_1(s) = s, T_j(s) = 2sT_{j-1}(s) - T_{j-2}(s),\ j = 2,3,\ldots;\ s \in [-1,1]$ are orthogonal base functions. These are the well-known Chebyshev polynomials and in our case $s = 2t-1$, since $t \in [0,1]$.

According to the theory, for the class of continuous functions on $[0,1]$ the element of best uniform approximation exists. Due to the equioscillation theorem, there are at least $(m+k+2)$ points $\{t_i^*\}_1^{m+k+2}$, where the error $r_\alpha^\beta(t) - t^{\beta-\alpha}$ have extremes and the sign alternates. We use orthogonal base functions, because there are numerical difficulties (instabilities) for finding r_α^β in the standard monomial basis $\{t^j\}$ (see [8]). The benefits of working in Chebyshev basis are illustrated in Table 5, where the maximal values of m and k for which the element of best uniform approximation of $t^{1-\alpha}$ can be successfully computed (the algorithm converges) are documented. The left pairs in the table correspond to best polynomial approximation ($k = 0$), while the right ones correspond to best (m,m)-rational approximation ($m = k$). It is evident that apart from the choice of base functions, calculations heavily depend on the used precision for arithmetic operations (single, double, quadruple). This is due to the non-differentiability of $t^{1-\alpha}$ at zero. The function is only $(1-\alpha)$-Hölder continuous (i.e. in $C^{0,1-\alpha}[0,1]$) and as a result most of the equi-oscillation points $\{t_i^*\}_1^{2m+2}$ of r_α^1 are clustered in a neighborhood of zero to account for the steep slope there. For example, when $m = 5$ and $\alpha = 0.75$ the first two points are $t_1^* = 0$ and $t_2^* \approx 3 \cdot 10^{-9}$, while the ninth point value is still just $t_9^* \approx 0.05$. Therefore, to accurately compute $\{t_i^*\}$ and capture the sign changes of $r_\alpha^1(t) - t^{1-\alpha}$ between them one must use high precision arithmetics.

Table 5. Maximal values (m,k) for which Algorithm 3.1 converges.

Precision	Base	$\alpha = 0.25$	$\alpha = 0.50$	$\alpha = 0.75$
Single	t^j	(8,0), (4,4)	(8,0), (4,4)	(8,0), (2,2)
Single	$T_j(s)$	(40,0), (3,3)	(50,0), (2,2)	(50,0), (2,2)
Double	t^j	(19,0), (6,6)	(19,0), (4,4)	(19,0), (2,2)
Double	$T_j(s)$	(60,0), (5,5)	(60,0), (5,5)	(50,0), (4,4)
Quadro	t^j	(35,0), (6,6)	(35,0), (4,4)	(35,0), (2,2)
Quadro	$T_j(s)$	(95,0), (11,11)	(95,0), (11,11)	(95,0), (7,7)

We suggest the following (modified Remez) algorithm for finding the β-BURA of $t^{\beta-\alpha}$ on $[0,1]$. To improve the stability of the approximation method we use the presentation (23), so that we work with the function $f(s) = \left(\frac{1+s}{2}\right)^{\beta-\alpha}$ for $s \in [-1,1]$ (see [17], [5]).

Algorithm 3.1. Input: (α,β), (m,k), N *(maximal number of algorithm iterations)*, V *(maximal number of inside iterations for solving the non-linear system in Step 3(ii))*, $\delta > 0$ *(accuracy)*. **Initialization:** ℓ, $s^{(0)}$, *and* $\bar{r}_0$, *satisfying*

- $\ell = m + k + 2$.
- $\left\{s_i^{(0)}\right\}_{i=1}^{\ell}$ – *strictly monotonically increasing sequence in* $[-1,1]$.
- $\bar{r}_0(s) = \frac{\bar{P}_m(s)}{\bar{Q}_k(s)}\ :\ \left(f(s_i^{(0)}) - \bar{r}_0(s_i^{(0)})\right)\ /\ \left(f(s_{i+1}^{(0)}) - \bar{r}_0(s_{i+1}^{(0)})\right) < 0,\ \forall i = 1,\ldots,\ell-1.$

FOR $n = 1, 2, \ldots$ **DO**

(1) Updating the equioscillation point set: *FOR* $i = 1, \ldots, \ell$ *DO*

(i) $\underline{\tau}_i^{(n)} := \sup_{-1 \le \tau \le s_i^{(n-1)}} \{f(\tau) = \bar{r}_{n-1}(\tau)\}, \qquad \bar{\tau}_i^{(n)} := \inf_{s_i^{(n-1)} \le \tau \le 1} \{f(\tau) = \bar{r}_{n-1}(\tau)\}.$

(ii) $s_i^{(n)} = \operatorname{argmax}_{\underline{\tau}_i^{(n)} \le s \le \bar{\tau}_i^{(n)}} |f(s) - \bar{r}_{n-1}(s)|, \qquad \eta_i^{(n)} = |f(s_i^{(n)}) - \bar{r}_{n-1}(s_i^{(n)})|.$ *END FOR*

(iii) $s_*^{(n)} = \operatorname{argmax}_{-1 \le s \le 1} |f(s) - \bar{r}_{n-1}(s)|, \qquad \eta_*^{(n)} = |f(s_*^{(n)}) - \bar{r}_{n-1}(s_*^{(n)})|.$

(iv) *IF* $\left(s_*^{(n)} \notin \{s_i^{(n)}\}_1^\ell\right)$ *THEN FIND* j *s.t.* $s_j^{(n)} < s_*^{(n)} < s_{j+1}^{(n)}$.
IF $\left(\operatorname{sgn}\left(f(s_*^{(n)}) - \bar{r}_{n-1}(s_*^{(n)})\right) = \operatorname{sgn}\left(f(s_j^{(n)}) - \bar{r}_{n-1}(s_j^{(n)})\right)\right)$ *THEN* $s_j^{(n)} = s_*^{(n)}$.
ELSE $s_{j+1}^{(n)} = s_*^{(n)}$.

(2) Convergence check: *IF* $\left(\max_i \eta_i^{(n)} - \min_i \eta_i^{(n)} < \delta\right)$ *OR* $(n = N + 1)$ **STOP**. *ELSE*

(3) Updating the rational approximation: *Solve iteratively the non-linear system*

$$\left(f\left(s_i^{(n)}\right) - \bar{r}_n\left(s_i^{(n)}\right)\right) = (-1)^i E_n, \qquad i = 1, \ldots, \ell$$

for the unknown E_n *and the coefficients of* $\bar{r}_n$*:*

(i) $(E_n^0\ ,\ \bar{r}_n^0) = (E_{n-1}\ ,\ \bar{r}_{n-1})$.

(ii) *FOR* $v = 1, 2, \ldots$ *DO: Solve the* $\ell \times \ell$ *linear system of equations*

$$\sum_{j=0}^{m} \bar{p}_j^{(n,v)} T_j(s_i^{(n)}) - \left(f(s_i^{(n)}) - (-1)^i E_n^{(v-1)}\right) \sum_{j=1}^{k} \bar{q}_j^{(n,v)} T_j(s_i^{(n)}) + (-1)^i E_n^{(v)} = f(s_i^{(n)}).$$

IF $\left|E_n^{(v)} - E_n^{(v-1)}\right| < \epsilon$, *OR* $v > V$ *GO to (iii). ELSE* $v = v + 1$ *and REPEAT.*

(iii) $\bar{r}_n(s) = \left(\sum_{j=0}^{m} \bar{p}_j^{(n,v)} T_j(s)\right) / \left(1 + \sum_{j=1}^{k} \bar{q}_j^{(n,v)} T_j(s)\right)$.

(iv) $E_n = E_n^{(v)}$.

(4) $n = n + 1$. *GO to Step 1.*

Output: n; $\quad \bar{r}_\alpha^\beta(s) = \bar{r}_n$; $\quad E_\alpha(m, k; \beta) = |E_n|$; $\quad s^* = \{s_i^{(n)}\}_{i=1}^\ell$.

Then we take $t^* = (s^* + 1)/2$ and get $r_\alpha^\beta(t)$ from $\bar{r}_\alpha^\beta(s)$ using (23).

Several remarks, concerning the computer implementation of the proposed algorithm are in order: (1) In the *Initialization* step, we usually take $s^{(0)}$ to be uniformly sampled on $[-1, 1]$, while for the derivation of an admissible $\bar{r}_0$ we apply least-squares optimization techniques. All the rational functions $\bar{r}_n$ are normalized with respect to the constant term in the denominator, i.e.,

$$\bar{r}_n(s) = \left(\sum_{j=0}^{m} \bar{p}_j^{(n)} T_j(s)\right) / \left(1 + \sum_{j=1}^{k} \bar{q}_j^{(n)} T_j(s)\right) \qquad \forall n \ge 0.$$

(2) In order to increase the computational efficiency of the algorithm, we compute neither the sequences $\underline{\tau}^{(n)}$ and $\bar{\tau}^{(n)}$ in *Step 1(i)* nor the local extrema $s^{(n)}$ in *Step 1(ii)*. Instead, we search for the maximal value of $|f(s) - \bar{r}_{n-1}(s)|$ on a small, discretized interval around $s_i^{(n-1)}$, decrease the mesh size, and repeat the process several times around the current maximizer. Such simple localization techniques seem to work fine for our numerical examples.

(3) In *Step 3(ii)* we apply Aitken-Steffensen acceleration but instead of $E_n^{(v-1)}$ for the system splitting we use a combination of the values$\{E_n^{(v-i)}\}_{i=1}^3$ from the previous three steps.

3.2. **Accuracy.** In this subsection we briefly discuss issues related to the numerical accuracy of the developed framework. We do not go into details, since thorough analysis of the algorithm is outside the scope of the paper. However, certain observations in this direction are worth mentioning, so that the reader can make conclusions for the full picture.

Theorem 2.1 quantifies the error between $\mathbf{u}_r = r_\alpha^\beta(\mathcal{A})\mathcal{A}^{-\beta}\mathbf{f}$ and $\mathbf{u} = \mathcal{A}^{-\alpha}\mathbf{f}$. All the estimations are under the assumption that $\mathbf{u}_r$ can be exactly computed by an optimal numerical solver. Within the adopted setup $m < k + \beta$ and $p_2 = 0$, $\mathbf{u}_r$ has the following representation

$$\mathbf{u}_r = \sum_{i=1}^{\beta} c_{0,i}\mathcal{A}^{-i}\mathbf{f} + \sum_{i=1}^{k} c_i(\mathcal{A} - d_i I)^{-1}\mathbf{f} := \sum_{i=1}^{\beta} c_{0,i}\mathbf{v}_{0,i} + \sum_{i=1}^{k} c_i\mathbf{v}_i, \tag{24}$$

which is a simplification of (13). The practical computation of $\mathbf{u}_r$ involves $k + \beta$ applications of a solver, that independently solves each of the involved large-scale linear systems with a right-hand-side $\mathbf{f}$. The numerical stability of each solution depends on the condition number of the underlined linear operator.

Remark 3.1. *The matrix $\mathcal{A} - d_i I$ is better conditioned than $\mathcal{A}$ whenever $d_i < 0$ or $d_i > \Lambda_1 + \Lambda_N$. If $d_i > \Lambda_1 + \Lambda_N$, the condition numler $\mathrm{k}(\mathcal{A} + d_i I)$ is uniformly bounded and depends only on d_i.*

Since we are interested in operators $\mathcal{A}$ which spectrum is normalized to lie inside $(0, 1]$, and is not well-separated from zero, in every numerical example we have $\Lambda_1 \approx 0$ and $\Lambda_N \approx 1$. The poles of r_α^β are outside of (a neighborhood of) the unit interval $[0, 1]$, therefore all the d_i's naturally satisfy the condition in Remark 3.1. Thus, the numerical computation $\mathbf{v}_i^{MG}$ of $\mathbf{v}_i = (\mathcal{A} - d_i I)^{-1}\mathbf{f}$, $i = 1, \ldots, k$ is a stable process.

When $\beta = 1$, using the notation (21), we observe that the most time-consuming procedure is the derivation of $\mathbf{v}_0^{MG}$ that corresponds to inverting $\mathcal{A}$ ($\mathbf{v}_0 = \mathcal{A}^{-1}\mathbf{f}$). In our numerical experiments, we use algebraic multigrid (AMG) [12] as a preconditioner in a CG method. The same preconditioner can be used to operators like $\mathcal{A} - d_i I$. In Section 2 we already observed that for $m = k$ all coefficients c_i are positive and sum to p_m/q_m, cf. (20). The ratio p_m/q_m increases with α (see Tables 2 - 4 for $m = k = 5$) but seems to always be $\mathcal{O}(1)$. Therefore, for this setting the accuracy of the numerical derivation of $\mathbf{u}_r^{MG}$ is proportional to the accuracy of inverting $\mathcal{A}$. Hence, numerics are trustworthy in general and unsubstantial additional errors for $\mathbf{u}_r^{MG} - \mathbf{u}$ are accumulated.

3.3. **More refined analysis in the case $\beta > 1$.** When $\beta > 1$, since $\mathrm{k}(\mathcal{A}^\beta) = \mathrm{k}(\mathcal{A})^\beta$, we need to find an approximate solution of a system with much worst condition number than the original system. This could cause loss of stability (or loss of accuracy). Since we solve $\mathcal{A}^\beta\mathbf{v} = \mathbf{f}$ iteratively via β consecutive applications of the AMG solver as a preconditioner for $\mathcal{A}$, we need to analyze the stability of such computational strategy.

Theorem 3.2. *Let $\mu, \nu, \varepsilon > 0$ be given and $\mathbf{v} = \mathcal{A}^{-n}\mathbf{f}$, where $n \geq 2$. Assume that $\mathbf{z}^{MG}$ is a numerical solution for $\mathbf{z} = \mathcal{A}^{-(n-1)}\mathbf{f}$, while $\mathbf{v}^{MG}$ is a numerical solution for $\bar{\mathbf{v}} = \mathcal{A}^{-1}\mathbf{z}^{MG}$. Then*

$$\frac{\|\mathbf{z}^{MG} - \mathbf{z}\|_{\mathcal{A}^{-1}}}{\|\mathbf{z}\|_{\mathcal{A}^{-1}}} \leq \mu\varepsilon, \quad \frac{\|\mathbf{v}^{MG} - \bar{\mathbf{v}}\|_{\mathcal{A}}}{\|\bar{\mathbf{v}}\|_{\mathcal{A}}} \leq \nu\varepsilon$$

imply

$$\frac{\|\mathbf{v}^{MG} - \mathbf{v}\|_{\mathcal{A}}}{\|\mathbf{v}\|_{\mathcal{A}}} \leq (\mu + \nu + \mu\nu\varepsilon)\,\varepsilon. \tag{25}$$

Proof. Applying triangle inequality, we derive

$$\begin{aligned}\|\mathbf{v}^{MG} - \mathbf{v}\|_{\mathcal{A}} \leq \|\mathbf{v}^{MG} - \bar{\mathbf{v}}\|_{\mathcal{A}} + \|\bar{\mathbf{v}} - \mathbf{v}\|_{\mathcal{A}} &\leq \nu\varepsilon\|\bar{\mathbf{v}}\|_{\mathcal{A}} + \|\bar{\mathbf{v}} - \mathbf{v}\|_{\mathcal{A}} \\ &\leq \nu\varepsilon\|\mathbf{v}\|_{\mathcal{A}} + (1 + \nu\varepsilon)\|\bar{\mathbf{v}} - \mathbf{v}\|_{\mathcal{A}};\end{aligned}$$

$$\|\bar{\mathbf{v}} - \mathbf{v}\|_{\mathcal{A}} = \|A^{-1}(\mathbf{z}^{MG} - \mathbf{z})\|_{\mathcal{A}} = \|\mathbf{z}^{MG} - \mathbf{z}\|_{\mathcal{A}^{-1}} \leq \mu\varepsilon\|\mathbf{z}\|_{\mathcal{A}^{-1}} = \mu\varepsilon\|\mathcal{A}\mathbf{v}\|_{\mathcal{A}^{-1}} = \mu\varepsilon\|\mathbf{v}\|_{\mathcal{A}}.$$

These imply $\|\mathbf{v}^{MG} - \mathbf{v}\|_{\mathcal{A}} \leq (\mu + \nu + \mu\nu\varepsilon)\,\varepsilon\|\mathbf{v}\|_{\mathcal{A}}$, which completes the proof. □

Note that $\mathbf{z}$ serves as a right-hand-side for the linear system $\mathcal{A}\mathbf{v} = \mathbf{z}$. Thus, for the stability in computing $\mathbf{v}$ the $\mathbf{z}$-related quantities need to be measured in the $\|\cdot\|_{\mathcal{A}^{-1}}$ norm.

Now we are ready to quantify the accuracy of the numerical derivation of $\mathbf{v}_{0,\beta} = \mathcal{A}^{-\beta}\mathbf{f}$ under the proposed above computational strategy. Iteratively, we define $\mathbf{v}_{0,1}^{MG}$ to be the output of the applied optimal solver (the notation MG doesn't mean that only multigrid solver can be used) to the linear system $\mathbf{v}_{0,1} = \mathcal{A}^{-1}\mathbf{f}$ and

$$\mathbf{v}_{0,j+1}^{MG} - \text{numerical solution of } \mathcal{A}\mathbf{v} = \mathbf{v}_{0,j}^{MG}, \qquad j = 1, \ldots, \beta - 1.$$

Corollary 3.3. *Let $\beta \geq 1$ and $\mathbf{v}_{0,\beta}^{MG}$ be derived as described above. Assume that a numerical solver for the system $\mathcal{A}\mathbf{v} = \mathbf{z}$, with arbitrary $\mathbf{v}, \mathbf{z} \in \mathbb{R}^N$ has computed $\mathbf{v}^{MG}$ with guaranteed relative error ε, i.e.*

$$\frac{\|\mathbf{v}^{MG} - \mathbf{v}\|_{\mathcal{A}}}{\|\mathbf{v}\|_{\mathcal{A}}} \leq \varepsilon.$$

Then

$$\frac{\|\mathbf{v}_{0,\beta}^{MG} - \mathbf{v}_{0,\beta}\|_{\mathcal{A}}}{\|\mathbf{v}_{0,\beta}\|_{\mathcal{A}}} \leq a_\beta \varepsilon, \quad \textit{with} \quad a_\beta = 1 + (1+\varepsilon)\mathrm{k}(\mathcal{A})a_{\beta-1}, \quad a_1 = 1.$$

Consequently, $a_\beta = \mathcal{O}(\mathrm{k}(\mathcal{A})^{\beta-1})$.

Proof. The proof is by induction. For $\beta = 1$, we have that $\mathbf{v}_{0,1}^{MG}$ is the solver output for $\mathbf{v}_{0,1} = \mathcal{A}^{-1}\mathbf{f}$. Thus, $a_1 = 1$ follows directly from the assumption on the solver accuracy. Now, let

$$\frac{\|\mathbf{v}_{0,\beta}^{MG} - \mathbf{v}_{0,\beta}\|_{\mathcal{A}}}{\|\mathbf{v}_{0,\beta}\|_{\mathcal{A}}} \leq a_\beta \varepsilon$$

holds true for β. Denote by $\bar{\mathbf{v}}_{0,\beta+1} := \mathcal{A}^{-1}\mathbf{v}_{0,\beta}^{MG}$. Again, due to the solver accuracy, we have

$$\frac{\|\mathbf{v}_{0,\beta+1}^{MG} - \bar{\mathbf{v}}_{0,\beta+1}\|_{\mathcal{A}}}{\|\bar{\mathbf{v}}_{0,\beta+1}\|_{\mathcal{A}}} \leq \varepsilon.$$

Applying the obvious inequalities $\Lambda_1^2\langle\mathcal{A}^{-1}\mathbf{v},\mathbf{v}\rangle \leq \langle\mathcal{A}\mathbf{v},\mathbf{v}\rangle \leq \Lambda_N^2\langle\mathcal{A}^{-1}\mathbf{v},\mathbf{v}\rangle$ we obtain

$$\frac{\|\mathbf{v}_{0,\beta}^{MG} - \mathbf{v}_{0,\beta}\|_{\mathcal{A}^{-1}}}{\|\mathbf{v}_{0,\beta}\|_{\mathcal{A}^{-1}}} \leq \frac{\Lambda_1^{-1}\|\mathbf{v}_{0,\beta}^{MG} - \mathbf{v}_{0,\beta}\|_{\mathcal{A}}}{\Lambda_N^{-1}\|\mathbf{v}_{0,\beta}\|_{\mathcal{A}}} \leq \mathrm{k}(\mathcal{A})\frac{\|\mathbf{v}_{0,\beta}^{MG} - \mathbf{v}_{0,\beta}\|_{\mathcal{A}}}{\|\mathbf{v}_{0,\beta}\|_{\mathcal{A}}} \leq \mathrm{k}(\mathcal{A})a_\beta\varepsilon.$$

The result follows from Theorem 3.2 which we apply with $\mu = \mathrm{k}(\mathcal{A})a_\beta$ and $\nu = 1$. □

The coefficient $c_{0,\beta} = \pm E_\alpha(m,k;\beta)$, due to (19). Therefore the numerical accuracy for the computation of the term $c_{0,\beta}\mathbf{v}_{0,\beta}$ in $\mathbf{u}_r$ (see (24)) depends on the product $E_\alpha(m,k;\beta)\mathrm{k}(\mathcal{A})^{\beta-1}$. For $\beta > 1$ this product contains two factors that behave differently when β grows: the first decreases (see, Table 1) while the second increases. As a result, we conclude that computing with $\beta = 1$ is a reasonable practical choice.

4. Numerical tests

A comparative analysis of the numerical accuracy of the proposed solvers and the related theoretical estimates are presented in this section. The first group of tests concerns matrices obtained from a three-point approximation of the Poisson equation in one space dimension. For this setting we are able to directly compute the exact solution $\mathbf{u} = \mathcal{A}^{-\alpha}\mathbf{f}$, as well as the approximate solution $\mathbf{u}_r = r_\alpha^\beta(\mathcal{A})\mathcal{A}^{-\beta}\mathbf{f}$, thus no additional numerical errors are accumulated in the process. The first experimental set is devoted to the numerical validation of Theorem 2.1. The second one studies possible improvements in the accuracy of the approximation $\mathbf{u}_r$ for larger α when a multi-step approximation process that involves smaller α's is applied. Finally, we run 3D numerical experiments, where $\mathbf{u}$ is unknown, while $\mathbf{u}_r$ is computed by a numerical solver that uses algebraic multigrid as a preconditioner in the conjugate gradient method.

In all the experiments we take $m + 1 = k + \beta$, thus we solve $m + 1$ linear systems in order to determine $\mathbf{u}_r$ (see (13)). We consider $m = \{5, 7\}$, $\beta = \{1, 2\}$, and $\alpha = \{0.25, 0.5, 0.75\}$. For

TABLE 6. Errors $E_\alpha(m, m+1-\beta;\beta)$ of BURA $P^*_m(t)/Q^*_{m+1-\beta}(t)$ of $t^{\beta-\alpha}$ on $[0,1]$.

α	$E_\alpha(5,5;1)$	$E_\alpha(5,4;2)$	$E_\alpha(5,3;3)$	$E_\alpha(7,7;1)$	$E_\alpha(7,6;2)$	$E_\alpha(7,5;3)$
0.75	2.7162E-3	3.8415E-6	4.6657E-7	7.8966E-4	2.0108E-7	6.6194E-9
0.50	2.6896E-4	2.0349E-6	4.0421E-7	4.6037E-5	7.8577E-8	4.3899E-9
0.25	2.8676E-5	6.2333E-7	1.8958E-7	3.2566E-6	1.8043E-8	1.5792E-9

each of the corresponding BURA functions all the zeros d_i of the denominator are real and of multiplicity one, so only systems of the type $(\mathcal{A}-d_iI)^{-1}\mathbf{f}$ appear. The approximation errors are summarized in Table 6. Detailed information about the BURA functions can be found in the Appendix through Tables 9-11. In the discussion below the Euclidean norm of a vector in $\mathbb{R}^N$ is denoted as ℓ^2-norm.

4.1. **Numerical validation of Theorem 2.1.** We consider the $N\times N$ stiffness matrix $\mathcal{A}$, corresponding to a three-point finite difference approximation (or FE approximation with linear elements) of the operator $\mathcal{L}u=-u''$ with zero Dirichet boundary conditions on a uniform partitioning of $(0,1)$ with mesh-size $h=1/(N+1)$. The tridiagonal matrix is normalized so that its spectrum lies inside $[0,1]$ and has enrties $1/2$ on the main diagonal and $-1/4$ on the upper and lower co-diagonals.

The eigenvalues and eigenvectors of $\mathcal{A}$ are

$$\Lambda_i=\sin^2\left(\frac{i\pi}{2(N+1)}\right),\qquad \mathbf{\Psi}_i=\left\{\sin\frac{ik\pi}{N+1}\right\}_{k=1}^{N},\qquad i=1,\dots,N.$$

Note that all the eigenvectors $\mathbf{\Psi}_i$ are of the same length, due to

$$\|\mathbf{\Psi}_i\|_2^2=\langle\mathbf{\Psi}_i,\mathbf{\Psi}_i\rangle=\sum_{k=1}^{N}\sin^2\frac{ik\pi}{N+1}=\frac{N}{2}-\frac{1}{2}\sum_{k=1}^{N}\cos\frac{2ik\pi}{N+1}=\frac{N+1}{2}$$

so we do not normalize them.

TABLE 7. Numerical error ε in (9) for $(m,k)=(5,5)$ and $\beta=1$. For each α the left column shows the results for $\mathbf{f}$ consisting of eigenvectors, while the right column is the error for $\mathbf{f}$ taken as 1000 random eigenvector combinations. In each box averaged error (top) and the maximal error (bottom) are reported.

h^{-1}	$\alpha=0.25$		$\alpha=0.5$		$\alpha=0.75$	
	$E_\alpha(5,5;1)=$**2.8676**E-05		$E_\alpha(5,5;1)=$**2.6896**E-04		$E_\alpha(5,5;1)=$**2.7162**E-03	
	$\{\mathbf{\Psi}_i\}_{i=1}^N$	rand1000	$\{\mathbf{\Psi}_i\}_{i=1}^N$	rand1000	$\{\mathbf{\Psi}_i\}_{i=1}^N$	rand1000
32	1.7187E-05	1.1682E-05	1.5982E-04	1.1223E-04	1.7361E-03	2.2177E-03
	2.8674E-05	2.3007E-05	2.6894E-04	2.2944E-04	2.7162E-03	2.5586E-03
64	1.7671E-05	1.3317E-05	1.6822E-04	1.5173E-04	1.7094E-03	1.4116E-03
	2.8675E-05	2.5055E-05	2.6873E-04	2.3036E-04	2.7143E-03	2.2590E-03
128	1.8185E-05	2.1587E-05	1.7122E-04	2.2000E-04	1.7215E-03	1.8407E-03
	2.8661E-05	2.4988E-05	2.6893E-04	2.5392E-04	2.7162E-03	2.3217E-03
256	1.8271E-05	2.1525E-05	1.7150E-04	2.0415E-04	1.7315E-03	2.2272E-03
	2.8675E-05	2.4464E-05	2.6896E-04	2.4437E-04	2.7160E-03	2.4607E-03

Numerical results for $m=5$, $\beta=1,2$ are summarized in Tables 7-8. As suggested by (9), in Table 7 we present the relative error $\|\mathbf{u}_r-\mathbf{u}\|_{\mathcal{A}}/\|\mathbf{f}\|_{\mathcal{A}^{-1}}$ while in Table 8 we show the relative error $\|\mathbf{u}_r-\mathbf{u}\|_{\mathcal{A}}/\|\mathbf{f}\|_{\mathcal{A}^{-3}}$. We use as input the coefficient vector of $\mathbf{f}$ with respect to the basis $\{\mathbf{\Psi}_i\}_{i=1}^N$, so the derivation of the exact solution $\mathbf{u}$ as well as the computation of the norms $\|\mathbf{f}\|_{\mathcal{A}^{-1}}$, respectively $\|\mathbf{f}\|_{\mathcal{A}^{-3}}$, is straightforward. In order to compute the approximated solution $\mathbf{u}_r$, we first generate the coefficient vector of $\mathbf{f}$ with respect to the standard basis $\{\delta_{ik}\}_{i,k=1}^N$ and then solve exactly the

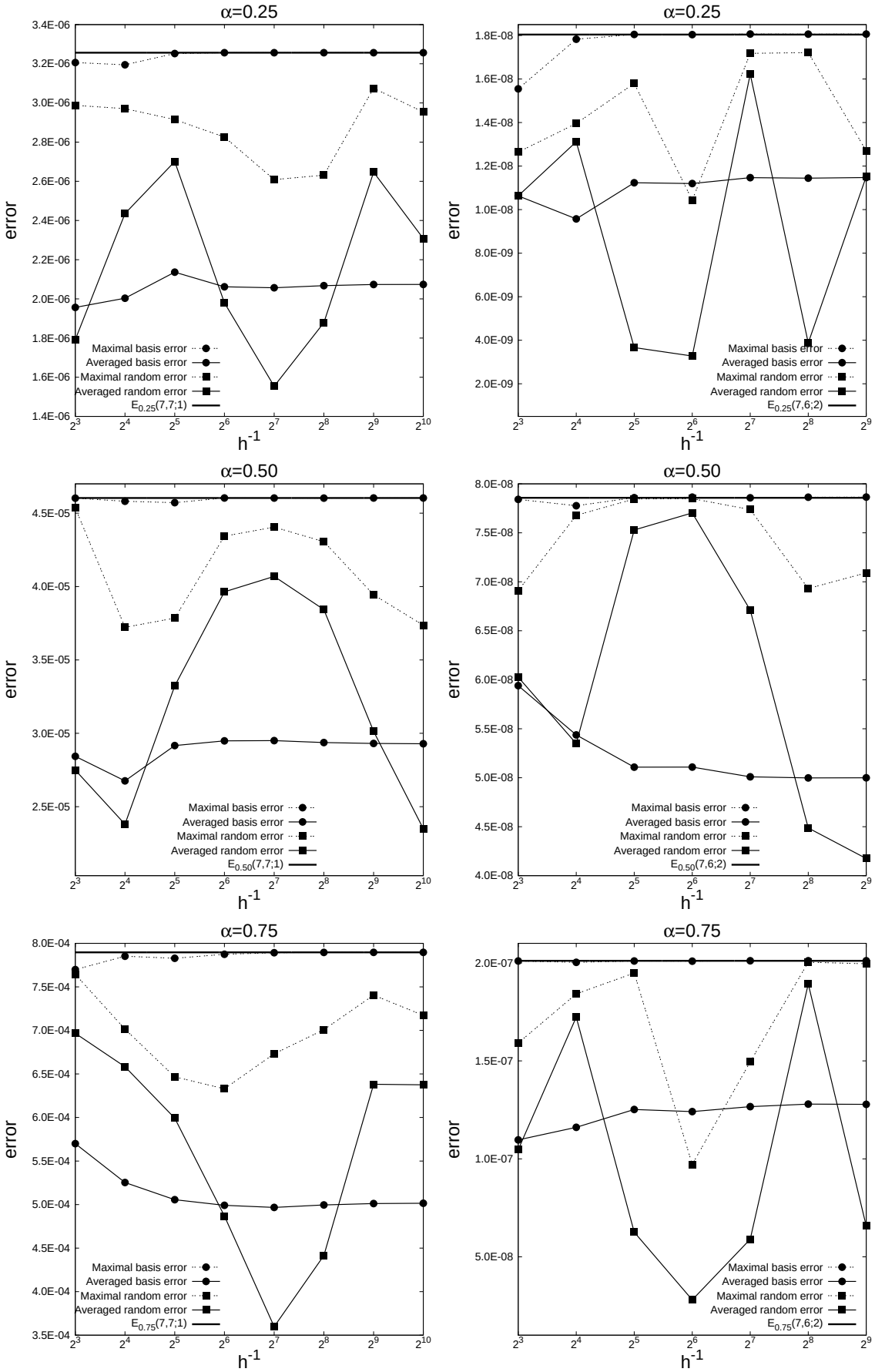

FIGURE 1. 1D numerical validation of Theorem 2.1 for $m = 7$. Left: $(7, 7; 1)$. Right: $(7, 6; 2)$. Error is measured as indicated in (9)

.

TABLE 8. Numerical error ε in (9) for $(m,k) = (5,4)$ and $\beta = 2$. For each α the left column shows the results for $\mathbf{f}$ consisting of eigenvectors, while the right column is the error for $\mathbf{f}$ taken as 1000 random eigenvector combinations. In each box averaged error (top) and the maximal error (bottom) are reported.

h^{-1}	$\alpha = 0.25$		$\alpha = 0.5$		$\alpha = 0.75$	
	$E_\alpha(5,4;2) =$**6.2333**E-07		$E_\alpha(5,4;2) =$**2.0349**E-06		$E_\alpha(5,4;2) =$**3.8415**E-06	
	$\{\mathbf{\Psi}_i\}_{i=1}^N$	rand1000	$\{\mathbf{\Psi}_i\}_{i=1}^N$	rand1000	$\{\mathbf{\Psi}_i\}_{i=1}^N$	rand1000
32	4.0549E-07	5.1262E-07	1.2511E-06	0.4000E-06	2.4108E-06	3.0845E-06
	6.2084E-07	6.1948E-07	2.0339E-06	1.6229E-06	3.8408E-06	3.3598E-06
64	3.9555E-07	3.5422E-07	1.2913E-06	1.7596E-06	2.4612E-06	3.5087E-06
	6.2311E-07	4.8304E-07	2.0345E-06	1.8513E-06	3.8412E-06	3.5512E-06
128	3.9521E-07	2.6196E-07	1.2864E-06	0.4378E-06	2.4346E-06	2.1079E-06
	6.2333E-07	5.8387E-07	2.0348E-06	1.8475E-06	3.8415E-06	3.5093E-06
256	3.9590E-07	4.8720E-07	1.2914E-06	1.2973E-06	2.4401E-06	1.4799E-06
	6.2332E-07	5.1011E-07	2.0349E-06	1.4255E-06	3.8414E-06	3.3265E-06

corresponding six tridiagonal linear systems that originate from the fractional decomposition of $t^{-\beta} r_\alpha^\beta(t)$. Randomness in the tables is with respect to the entries of the input coefficient vector.

We measure four different error quantities: the maximal error over the eigenvectors $\{\mathbf{\Psi}_i\}_{i=1}^N$, which coincides with the true estimate of the approximation error; the maximal error over the randomized set of $\mathbf{f}$'s, which is the numerical approach for estimating the former; the averaged error over the eigenvectors; and the averaged error over the random right-hand-side set. The last two quantities provide information about the general behavior of the error and its expectation value. The main observation is that the errors, related to the eigenvectors set behave quite stably with respect to the size of $\mathcal{A}$, unlike the errors related to random vector input. Such "dimension-invariance" of the results from the first class is due to the almost uniform distribution of the eigenvalues $\{\Lambda_i\}_{i=1}^N$ of $\mathcal{A}$ along the interval $[0,1]$ and that for every β-BURA function the endpoints 0 and 1 are maximal oscillation points for the residual $r_\alpha^\beta(t) - t^{\beta-\alpha}$ (i.e., $\{0,1\} \subset \{t_i^*\}_1^{m+k+2}$). As $N \to \infty$, we have $\Lambda_1 \to 0$, $\Lambda_N \to 1$ and we observe that all the maximal norm ratio errors for eigenvectors input tend to the corresponding univariate error $E_\alpha(m,k;\beta)$. The β-BURA functions oscillate mainly close to a similar behavior there and is stable close to 1, making $|r_\alpha^\beta(\Lambda_N) - \Lambda_N^{\beta-\alpha}| \to E_\alpha(m,k;\beta)$ quickly. Therefore, the placement of the remaining spectrum $\{\Lambda_i\}_{i=1}^{N-1}$ of $\mathcal{A}$ with respect to $\{t_i^*\}$ is not significant for the close relation between the theoretical error value ε in (9) and the univariate error ε in (6). On the other hand, it is practically impossible to generate (a rescaled version of) $\mathbf{\Psi}_N$ at random, so the randomized errors heavily depend on the placement of the whole spectrum of $\mathcal{A}$ with respect to the maximal oscillating points of the β-BURA function. As a result, both maximal and averaged random error can be anywhere in the interval between the minimal and maximal error of the eigenvectors. We generated various random sets of different size (e.g., $10^3, 10^4$) and checked that for a fixed N the two errors behave stably with respect to the choice of randomness. This allows us to conclude that the "dimension-instability" phenomenon is indeed fully due to the specifics of the spatial distribution of the spectrum of $\mathcal{A}$.

Similar observations and the same conclusions can be drawn from the second experimental set that corresponds to $m = 7$. The errors are illustrated on Fig. 1 and documented in Tables 12-13 in the Appendix. The only difference, worth mentioning, is the accumulation of additional numerical errors in the computation of the partial fraction decomposition of $t^{-\beta} r_\alpha^\beta(t)$ due to the usage of unsatisfactory precision for the recording of the poles $\{d_i\}$ of r_α^β. Indeed, we used precision 10^{-9} which affected the accuracy of the computation of $t^{-\beta} r_\alpha^\beta(t)$ as confirmed by the results in Table 13.

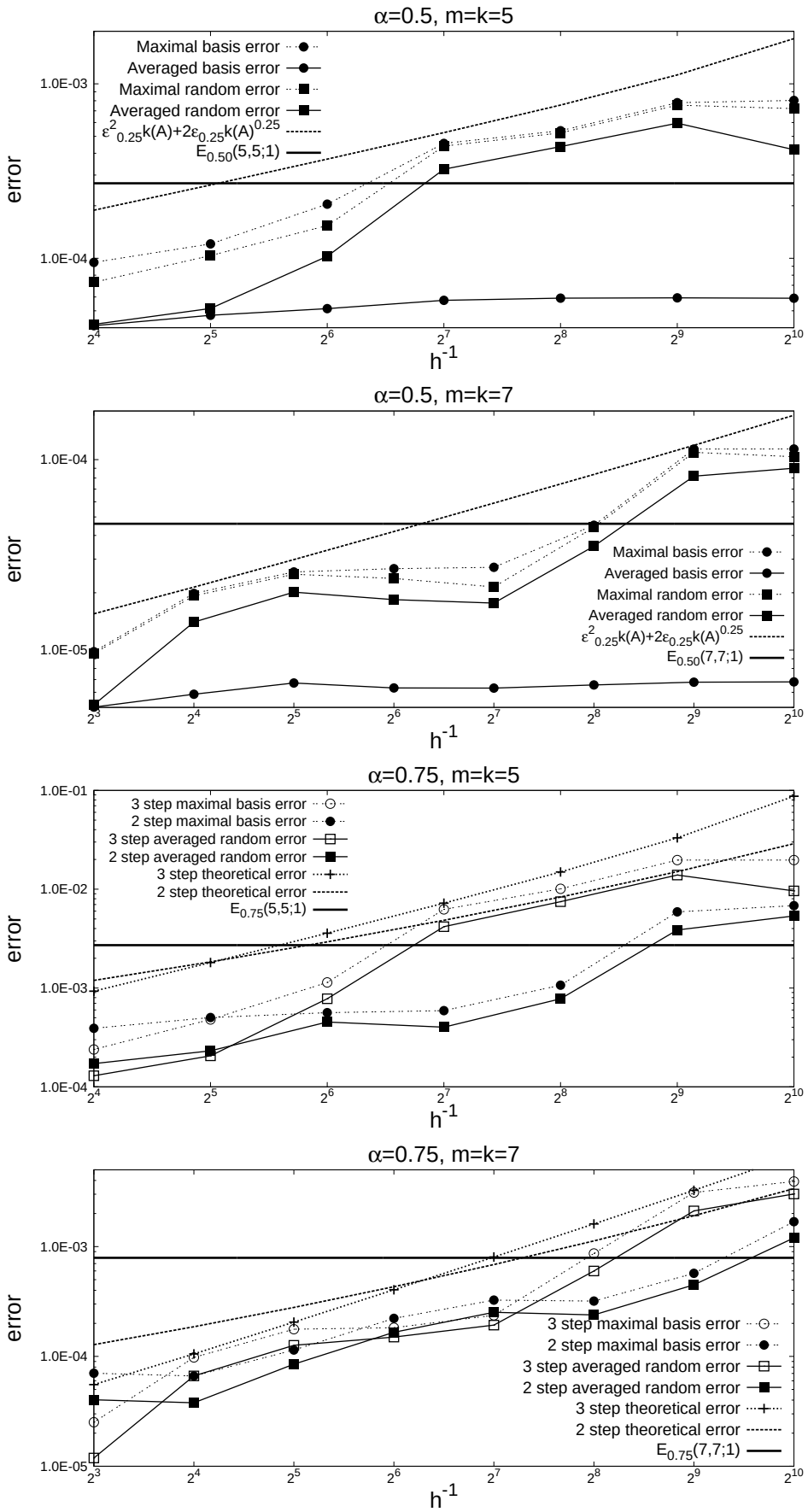

FIGURE 2. Numerical error the one-dimensional problem for the multi-step case. The relative errors $\|\mathbf{u}_r - \mathbf{u}\|_{\mathcal{A}}/\|\mathbf{f}\|_{\mathcal{A}^{-1}}$ are plotted.

4.2. **Multi-step 1-BURA approximation for $\alpha = \{0.5, 0.75\}$.** From Table 1 we observe that when α increases, so does the error $E_\alpha(m, m; \beta)$. In particular, for $\beta = 1$, the quantities $E_{0.25}(m, m; 1)$, $E_{0.50}(m, m; 1)$ and $E_{0.75}(m, m; 1)$ are all of different order. This is due to the steeper slopes in a neighborhood of zero for the function $t^{1-\alpha}$, which results in higher and more frequent oscillations of the residual $r^1_\alpha(t) - t^{1-\alpha}$ there. Apart from such theoretical drawbacks, there are also additional numerical difficulties with the convergence of Algorithm 3.1 as the set of maximal oscillation points $\{t^*_i\}_1^{2m+2}$ for the residual cluster around zero. Indeed, higher numerical precision is needed for the correct separation of the oscillating points, as well as more internal and external iterations are executed for solving the ill-conditioned linear systems in Step 3(ii) and for reaching the stopping criterion of the Algorithm, respectively. The second series of numerical experiments are devoted to circumventing the problem. Here, we study the possibility to replace the action of r^1_α by the joint action of several $r^1_{\alpha_i}$ rational functions, where each α_i is smaller than the original α, thus $r^1_{\alpha_i}$ is cheaper to be generated and its approximation error $E_{\alpha_i}(m.m; 1)$ is smaller.

Our idea is to apply a multi-step procedure, based on the identity

$$\mathcal{A}^{-\alpha}\mathbf{f} = \mathcal{A}^{-\alpha_n} \circ \mathcal{A}^{-\alpha_{n-1}} \circ \cdots \circ \mathcal{A}^{-\alpha_1}\mathbf{f}, \qquad \sum \alpha_i = \alpha.$$

First, we approximate $\mathcal{A}^{-\alpha_1}\mathbf{f}$ by $\mathbf{u}_1 := r^1_{\alpha_1}(\mathcal{A})\mathcal{A}^{-1}\mathbf{f}$. Then we approximate $\mathcal{A}^{-\alpha_2} \circ \mathcal{A}^{-\alpha_1}\mathbf{f}$ by $\mathbf{u}_2 := r^1_{\alpha_2}(\mathcal{A})\mathcal{A}^{-1}\mathbf{u}_1$ and so on. Finally, we approximate $\mathbf{u} = \mathcal{A}^{-\alpha}\mathbf{f}$ by $\mathbf{u}_n = r^1_{\alpha_n}(\mathcal{A})\mathcal{A}^{-1}\mathbf{u}_{n-1}$. Following (9) we are interested in the theoretical and numerical behavior of the error ratio $\|\mathbf{u}_n - \mathbf{u}\|_{\mathcal{A}}/\|\mathbf{f}\|_{\mathcal{A}^{-1}}$.

The theoretical error analysis is based on Theorem 2.1. Denote by $\varepsilon_i(t)$ the residual of $r^1_{\alpha_i}(t)$ with respect to $t^{1-\alpha_i}$. Then, for each $i = 1, \ldots, n$ we have

$$r^1_{\alpha_i}(t) = t^{1-\alpha_i} + \varepsilon_i(t), \qquad |\varepsilon_i(t)| \le E_{\alpha_i}(m, m; 1) \quad \forall t \in [0, 1]. \tag{26}$$

The multi-step approximation $\mathbf{u}_n$ can be rewritten in the form

$$\mathbf{u}_n = \prod_{i=1}^{n} r^1_{\alpha_i}(\mathcal{A})\, \mathcal{A}^{-n}\mathbf{f} = \left(\mathcal{A}^{n-1} \prod_{i=1}^{n} r^1_{\alpha_i}(\mathcal{A})\right) \mathcal{A}^{-1}\mathbf{f}.$$

Therefore the proof of Theorem 2.1 implies that we need to estimate the approximation error

$$E_{\alpha_1 \ldots \alpha_n}(m, m; 1) := \max_{t \in \{\Lambda_i\}_1^N} \left| \frac{r^1_{\alpha_1}(t) r^1_{\alpha_2}(t) \ldots r^1_{\alpha_n}(t)}{t^{n-1}} - t^{1-\alpha} \right|. \tag{27}$$

Consider $n = 2$. Using (26) we obtain

$$\frac{r^1_{\alpha_1}(t) r^1_{\alpha_2}(t)}{t} = t^{1-\alpha} + t^{-\alpha_1}\varepsilon_2(t) + t^{-\alpha_2}\varepsilon_1(t) + t^{-1}\varepsilon_1(t)\varepsilon_2(t).$$

Denote by $E_{\alpha_i} = E_{\alpha_i}(m, m; 1)$, $i = 1, 2$. Since the spectrum of $\mathcal{A}$ is normalized and $\Lambda_N = 1$, so that $t^{-\alpha_i} \le \Lambda_1^{-\alpha_i} = k(\mathcal{A})^{\alpha_i}$ and from (27) we conclude

$$E_{\alpha_1 \alpha_2}(m, m; 1) \le E_{\alpha_2} \mathrm{k}(\mathcal{A})^{\alpha_1} + E_{\alpha_1} \mathrm{k}(\mathcal{A})^{\alpha_2} + E_{\alpha_1} E_{\alpha_2} \mathrm{k}(\mathcal{A}). \tag{28}$$

Comparing with the error estimate $E_\alpha(m, m; 1)$ we observe that unlike the direct approach, the two-step approximation error depends on the condition number of $\mathcal{A}$, thus is not dimension-invariant in general. Therefore, the benefits from the proposed multi-step procedure for computing $\mathcal{A}^{-\alpha}\mathbf{f}$ are limited since the overall error is magnified by the condition number of $\mathcal{A}$.

The presented numerical experiments for $\mathcal{A} = tridiag(-0.25, 0.5, -0.25)$ as in Section 4.1, $m = \{5, 7\}$ and $\alpha = \{0.5, 0.75\}$ confirm the above theoretical analysis. The related results are summarized in Fig. 2. When $\alpha = 0.5$, we study the two step procedure based on $\alpha_1 = \alpha_2 = 0.25$. When $\alpha = 0.75$, we investigate both the two step procedure with $(\alpha_1, \alpha_2) = (0.5, 0.25)$ and the three step procedure based on $\alpha_1 = \alpha_2 = \alpha_3 = 0.25$. In the latter case, it is straightforward to derive the three-step analogous formula to (28), which in the particular setup implies

$$E_{0.25\,0.25\,0.25}(m, m; 1) = E^3_{0.25} \mathrm{k}^2(\mathcal{A}) + 3E^2_{0.25} \mathrm{k}^{5/4}(\mathcal{A}) + 3E_{0.25} \mathrm{k}^{1/2}(\mathcal{A}). \tag{29}$$

Again, as in (28), we use the short notation $E_{0.25}$ for $E_{0.25}(m, m; 1)$.

We set $h^{-1} = N + 1 = 2^i$, $i \in \{3, 4, \dots, 10\}$ and plot various errors. Namely, for $\alpha = 0.5$ those are: the theoretically estimated two-step error (28), the true two-step error estimate that coincides with the maximal error over the eigenvectors $\{\mathbf{\Psi}_i\}_{i=1}^N$, the averaged two-step error over the eigenvectors, the maximal and averaged two-step errors over a thousand randomly generated vectors, and the one-step error $E_{0.50}(m, m; 1)$. For $\alpha = 0.75$ we plot the theoretically estimated two and three step errors (28)-(29), the true two and three step error estimates, the corresponding averaged errors of random right-hand-side data, and the one-step error $E_{0.75}(m, m; 1)$. All the derived numerical results are documented in Tables 14-15 in the Appendix.

From the plots in Fig. 2 we observe that when the α_i's coincide the true multi-step error estimate reaches the theoretical bound for particular sizes of $\mathcal{A}$. This happens when Λ_1 hits a maximal oscillation point of $r^1_{0.25}$, i.e., $|r^1_{0.25}(\Lambda_1) - \Lambda_1^{3/4}| \approx E_{0.25}$, as for $h = 2^{-7}$, $m = 5$ and $h = \{2^{-4}, 2^{-9}\}$, $m = 7$. When $\alpha_1 \neq \alpha_2$ we observe that the theoretical bound $E_{0.25\,0.50}$ is an overestimation of the true maximal error, since the sets of internal maximal oscillation points for $r^1_{0.25}$ and $r^1_{0.50}$ are disjoint and it is not possible for Λ_1 to simultaneously hit both. Note that Λ_1 tends to zero as $N \to \infty$ but it never reaches zero and the heavy oscillations of the residual in this area do not allow the maximal basis error to reach $E_{0.25\,0.50}$ even for $\mathcal{A}$ of size 1023×1023.

Unlike the first experimental setup, here we witness similar behavior among the true error, the maximal random error, and the averaged random error, meaning that the measured quantity is stable and does not heavily depend on $\mathbf{f}$. This is due to the specifics of the multi-step procedure and the existence of pole at zero for the product rational approximation. Hence, whenever $\langle \mathbf{f}, \mathbf{\Psi}_1 \rangle \neq 0$ this component dominates the overall error value. Because of that, the averaged basis error do not provide reliable information about the error in the general (worst) case, since the eigenvectors of $\mathcal{A}$ are mutually orthogonal. This error remains substantially below the one-step error $E_{0.50}$ in all conducted experiments.

As m increases, the two-step error remains better than the one-step error for a larger set of matrix sizes. For $\alpha = 0.5$ and $m = 5$ the two-step error overpasses $E_{0.50}$ for $h = 2^{-7}$, while for $m = 7$ this happens for $h = 2^{-9}$. For $\alpha = 0.75$ the benefits of the two-step process are bigger, as the two-step error remains in vicinity of $E_{0.75}$ even for $h = 2^{-10}$. However, as in the theoretical analysis, we clearly see the dimension-dependence of the multi-step errors. Nevertheless, with respect to controlling the ratio $\|\mathbf{u}_r - \mathbf{u}\|_{\mathcal{A}} / \|\mathbf{f}\|_{\mathcal{A}^{-1}}$ in the cases when r^1_α cannot be numerically computed, the proposed two-step procedure seems a better choice than r^2_α asymptotically, since

$$\frac{\|r^2_\alpha(\mathcal{A})\mathcal{A}^{-2}\mathbf{f} - \mathcal{A}^{-\alpha}\mathbf{f}\|_{\mathcal{A}}}{\|\mathbf{f}\|_{\mathcal{A}^{-1}}} \leq \frac{\|r^2_\alpha(\mathcal{A})\mathcal{A}^{-2}\mathbf{f} - \mathcal{A}^{-\alpha}\mathbf{f}\|_{\mathcal{A}}}{\|\mathbf{f}\|_{\mathcal{A}^{-3}}} \mathrm{k}(\mathcal{A}) \leq E_\alpha(m, m; 2)\mathrm{k}(\mathcal{A})$$

and, comparing to (28), we experimentally observe that $E_{\alpha_1}(m, m; 1)E_{\alpha_2}(m, m; 1) < E_\alpha(m, m; 2)$ if $\alpha_1 + \alpha_2 = \alpha$.

4.3. **Tests with approximate solving of $\mathcal{A}\mathbf{u}_e = \mathbf{f}$ by PCG method.** In higher spatial dimensions, when the domain Ω in (3) is a subset of $\mathbb{R}^d$, $d > 1$, and we cannot compute the exact solution $\mathbf{u} = \mathcal{A}^{-\alpha}\mathbf{f}$. In general, we don't have explicitly the eigenvalues and eigenvectors of $\mathcal{A}$. Thus, in the analysis of the numerical tests, we cannot apply error estimates of the form (9). In order to numerically validate our theoretical estimates we use the two-step procedure from Section 4.2 through the following obvious identity

$$\mathbf{f} = \mathcal{A}\left(\mathcal{A}^{-(1-\alpha)}\left(\mathcal{A}^{-\alpha}\mathbf{f}\right)\right), \tag{30}$$

that holds true for an arbitrary vector $\mathbf{f} \in \mathbb{R}^N$. In (28) we argued that taking a product of two rational functions as an approximation of $t^{\beta-\alpha}$ with $\beta = 1$ the corresponding approximation error depends on the condition number of $\mathcal{A}$. For the multivariate validation of Theorem 2.1 such dimension-dependence is not acceptable, so we choose $\beta = 2$ here. In particular, we treat $r^1_{1-\alpha}r^1_\alpha$ as a 2-uniform rational approximation (this is not BURA, since the approximation error is not optimal) for the function $t^{2-1} = t$ on the unit interval $(0, 1]$. Applying (15) with $\gamma = 2$ we deduce

$$\|r^1_{1-\alpha}(\mathcal{A})r^1_\alpha(\mathcal{A})\mathcal{A}^{-2}\mathbf{f} - \mathcal{A}^{-1}\mathbf{f}\|_{\mathcal{A}^2} \leq E_{1-\alpha,\alpha}(m, m; 2)\|\mathbf{f}\|_{\mathcal{A}^{-2}}. \tag{31}$$

To avoid additional numerical inaccuracies, it is more convenient from a computational point of view to introduce the approximation vector $\mathbf{f}_r$ of $\mathbf{f}$ in (30), i.e.,

$$\mathbf{f}_r = \mathcal{A}\Big(r^1_{1-\alpha}(\mathcal{A})r^1_{\alpha}(\mathcal{A})\mathcal{A}^{-2}\mathbf{f}\Big) := \mathcal{A}\mathbf{u}_r.$$

Then we can rewrite the estimate (31) in the form

$$\|\mathbf{f}_r - \mathbf{f}\|/\|\mathcal{A}^{-1}\mathbf{f}\| \leq E_{1-\alpha,\alpha}(m,m;2). \tag{32}$$

We estimate the two-step error $E_{1-\alpha,\alpha}(m,m;2)$ with the help of (26), as in (27). The function $r^1_{1-\alpha}r^1_{\alpha}$ has no poles in $[0,1]$, thus we need not restrict ourselves to the spectrum of $\mathcal{A}$:

$$\begin{aligned} E_{1-\alpha,\alpha}(m,m;2) &= \max_{t\in[0,1]} |r^1_{1-\alpha}(t)r^1_{\alpha}(t) - t| = \max_{t\in[0,1]} |t^{\alpha}\varepsilon_{\alpha}(t) + t^{1-\alpha}\varepsilon_{1-\alpha}(t) + \varepsilon_{\alpha}(t)\varepsilon_{1-\alpha}(t)| \\ &\leq E_{1-\alpha}(m,m;1) + E_{\alpha}(m,m;1) + E_{1-\alpha}(m,m;1)E_{\alpha}(m,m;1). \end{aligned}$$

In practice, however, we observe that the residuals ε_{α} and $\varepsilon_{1-\alpha}$ are negative and monotonically decreasing in $[0.8,1]$. Due to this sign pattern and the fact that $\varepsilon_{\alpha}(1) = -E_{\alpha}$, $\varepsilon_{1-\alpha}(1) = -E_{1-\alpha}$ we can improve the two-step error estimate and conclude that:

$$\|\mathbf{f}_r - \mathbf{f}\|/\|\mathcal{A}^{-1}\mathbf{f}\| \leq E_{1-\alpha} + E_{\alpha} - E_{1-\alpha}E_{\alpha}. \tag{33}$$

The last estimate has been numerically confirmed as sharp for $m = \{5,7\}$ (see Tables 16-17 in the Appendix). Inspecting closely the above proof, we realize that the two-step residual is of order $E_{1-\alpha}E_{\alpha}$ or lower around zero. Furthermore, unlike the equioscillation BURA setting for the one-step process, the two-step residual reaches its maximum in absolute value only at $t = 1$ and the amplitudes of its other oscillations gradually decrease as t approaches zero. As a result, the numerically computed values for the maximal and averaged random errors w.r.t. (33) are closer to $E_{1-\alpha}E_{\alpha}$ than to $E_{1-\alpha} + E_{\alpha}$, meaning that the typical error is significantly smaller than the worst case scenario $E_{1-\alpha,\alpha}$.

We investigate two particular choices for $\mathbf{f}$, namely $\mathbf{f}^1 = (1,\ldots,1)$ and $\mathbf{f}^0 = (1,0,\ldots,0)$. In the case of one-dimensional elliptic problems (1D) $\mathcal{A} = tridiag(-0.25, 0.5, -0.25)$ and we exactly solve the corresponding linear systems. In 3D, we use the finite element method in space with linear conforming tetrahedral finite elements and an algebraic multigrid (AMG) preconditioner in the PCG solutions of the corresponding linear systems. To be more precise, the BoomerAMG implementation, e.g. [12], is used in our numerical tests. $\mathcal{A}$ is the stiffness matrix from the FE discretization of the problem (3) in $\Omega = [0,1]^3$ with $\mathbf{a} = a(x)I$, where I the identity matrix in $\mathbb{R}^d$ and $a(x)$ is a piece-wise constant function in Ω. In this case the jump of $a(x)$ is introduced via a scaling factor $0 < \mu \leq 1$.

The motivation for choosing these particular $\mathbf{f}$'s comes from the 1D case. Since for $i = 1,\ldots,N$

$$\langle \mathbf{\Psi}_i, \mathbf{f}^1\rangle = \begin{cases} 0, & i \text{ is even} \\ \cot(i\pi h/2), & i \text{ is odd} \end{cases} \qquad \langle \mathbf{\Psi}_i, \mathbf{f}^0\rangle = \sin(i\pi h) = \mathbf{\Psi}_{1,i},$$

so that we have the following representation of $\mathbf{f}^1$ and $\mathbf{f}^0$ by the eigen-vectors $\{\mathbf{\Psi}_i\}_{i=1}^N$

$$\mathbf{f}^1 = \sum_{i \text{ is odd}} 2h\cot(i\pi h/2)\mathbf{\Psi}_i = \sum_{i \text{ is even}} \frac{4}{i\pi}\frac{i\pi h/2}{\tan(i\pi h/2)}\mathbf{\Psi}_i; \quad \mathbf{f}^0 = \sum_{i=1}^{N} 2h\sin(i\pi h)\mathbf{\Psi}_i. \tag{34}$$

Therefore, from $x/\tan(x) < 1$ in $(0,\pi/2)$, we derive that the coefficients in the $\mathbf{f}^1$-decomposition (34) rapidly decay as i increases, meaning that the $\mathbf{\Psi}_1$ component dominates and the two-step residual at Λ_1 determines the behavior of the error ratio $\|\mathbf{f}^1_r - \mathbf{f}^1\|/\|\mathcal{A}^{-1}\mathbf{f}^1\|$. To summarize

$$\|\mathbf{f}^1_r - \mathbf{f}^1\|/\|\mathcal{A}^{-1}\mathbf{f}^1\| \approx \left|r^1_{1-\alpha}(\Lambda_1)r^1_{\alpha}(\Lambda_1) - \Lambda_1\right| \xrightarrow[h\to 0]{} E_{1-\alpha}E_{\alpha}. \tag{35}$$

Such asymptotic behavior of the ℓ^2-norm error ratio of $\mathbf{f}^1$ is numerically confirmed by the conducted 1D and 3D numerical experiments with $m = \{5,7\}$ and $\alpha = \{0.25, 0.5\}$, as illustrated on the left of Fig. 3. In 3D we run simulations up to $h = 2^{-8}$, which corresponds to $N = 6(h^{-1}+1)^3$, while in 1D we go up to $h = 2^{-20}$, and corresponding number of degrees of freedom $N = h^{-1}+1$.

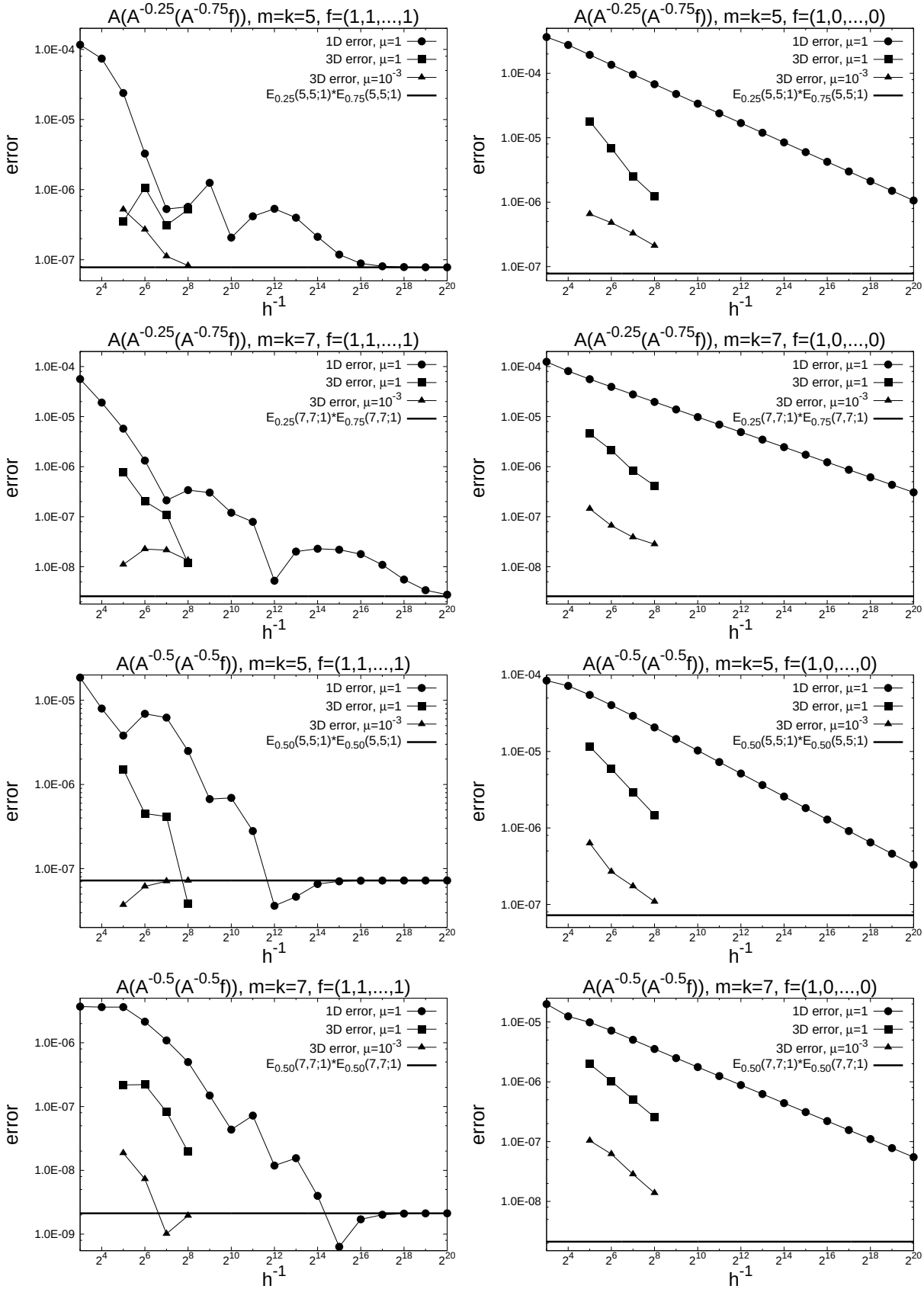

FIGURE 3. 1D and 3D numerical errors. Left: $\mathbf{f}^1 = (1, 1, \ldots, 1)$. Right: $\mathbf{f}^0 = (1, 0, \ldots, 0)$. The relative errors $\|\mathbf{f}_r - \mathbf{f}\|/\|\mathcal{A}^{-1}\mathbf{f}\|$ are plotted.

Clearly, the error tends to $E_{1-\alpha}E_\alpha$ as $\Lambda_1 \to 0$. We observe that in the 3D case with homogeneous coefficient ($\mathcal{L}$ is the Laplacian) the error for mesh-size $h^{-1} \in [2^6, 2^8]$ mimics the 1D error for mesh-size $h^{-1} \in [2^9, 2^{12}]$. For the heterogeneous 3D case, when in a half the unit cube the diffusion coefficients are scaled by $\mu = 10^{-3}$, $\mathrm{k}(\mathcal{A})$ is increased (approximately) by a factor of μ^{-1}, implying that Λ_1 is closer to zero than in the homogeneous case. As a result, the 3D error for the mesh-size $h^{-1} \in [2^6, 2^8]$ mimics the 1D error for the mesh-size $h^{-1} \in [2^{14}, 2^{17}]$.

The coefficients in the $\mathbf{f}^0$-decomposition (34) have symmetry due to the relations $2h\sin(i\pi h) = 2h\sin((N+1-i)\pi h$ with $h = 1/(N+1)$. Unlike for $\mathbf{f}^1$ case, the contribution of $\mathbf{\Psi}_1$ here is negligible and the behavior of the relative error $\|\mathbf{f}_r^0 - \mathbf{f}^0\|/\|\mathcal{A}^{-1}\mathbf{f}^0\|$ is dominated by the error $|r^1_{1-\alpha}(0.5)r^1_\alpha(0.5) - 0.5|$. This effect weakens with $h \to 0$, because the coefficients depend on the mesh-size and their distribution spreads away (standard deviation increases) when the grid is refined. The two-step residual is stable around $t = 1/2$ and the coefficients decay proportionally to the refinement scale, which results in monotone linear behavior of the error as a function of h^{-1}. The numerical results perfectly agree with this argument and, similar to the 1D-3D correspondence for $\mathbf{f}^1$, we observe that the slope of the error decay is steeper in 3D and the error decreases in the case of piece-wise constant coefficient $\mathbf{a}(x)$.

In the presented numerical tests, as a stopping criteria for the BoomerAMG PCG solver we have used a relative error less or equal to 10^{-12}. However, we want to note that the numerical results are practically not affected by using stopping criteria 10^{-6}, instead. Furthermore, for precision 10^{-12} the order of applying the 1-BURA functions $r^1_{0.25}$ and $r^1_{0.75}$ (i.e., taking $\alpha = 0.25$ or $\alpha = 0.75$ first) seems irrelevant and the corresponding relative errors have the same first five meaningful digits. This implies that the main numerical difficulties are related to the performance of Algorithm 3.1 and the correctness of the subsequent representation of r^β_α as a sum of partial fractions.

5. Concluding remarks

In this paper we propose algorithms of optimal complexity for solving the linear algebraic system $\mathcal{A}^\alpha\mathbf{u} = \mathbf{f}$, $0 < \alpha < 1$, where $\mathcal{A}$ is an SPD matrix obtained after discretization of a second order elliptic problem by a finite difference or finite elements method. Since the matrix $\mathcal{A}^\alpha$ is dense we approximate the above problem by to solving several systems with sparse SPD matrices of the form $\mathcal{A} + c\mathcal{I}$, $c \geq 0$. For this we use BoomerAMG, which has optimal complexity.

The method is based on best uniform rational approximations (BURA) of $t^{\beta-\alpha}$ for $0 < t \leq 1$ and natural β. Bigger β means stronger regularity assumptions and this is the reason to concentrate our considerations mostly to the cases $\beta \in \{1, 2\}$. Depending on α, β and the degrees of BURA (m, m) we got a relative accuracy of the method between $O(10^{-3})$ and $O(10^{-7})$ for $m \in \{5, 6, 7\}$.

Some computational limitations of the proposed approach were indicated in Table 5. The developed algorithm and code for finding the BURA for larger values of (m, m) faces problems related to the computer precision of arithmetic operations. Some improvements in this respect could be achieved by a proper local mesh refinement or/and rescaling of the parameter $t \in (0, 1]$.

In general, problems with fractional power of the elliptic operator show decrease in the regularity of the solution with decreasing of α. Thus, the finite elements solution of such problems will have lower accuracy compared to the finite element solution of the elliptic problem (no fractional powers involved). For instance, the following estimate has been proven in [3, Theorem 6.2]: $||(\mathcal{L}^{-\alpha} - \mathcal{L}_h^{-\alpha}\pi_h)f||_{L_2} \leq Ch^{2\sigma}||f||_{\dot{H}^{2\delta}}$, where π_h is the L^2 projection onto the finite element space, $\mathcal{L}_h$ is the finite element approximation of $\mathcal{L}$, σ characterizes the elliptic regularity (it is determined in [3, Assumption 1] as lifting the data $f \in H^{-1+\sigma}$ by $\mathcal{L}^{-1}$ to $H^{1+\sigma}$), and $\delta > \sigma - \alpha$. Now, in the context of this paper, the question about using and justifying theoretically proper norms of the error is very important, but not considered. A study of this issue needs a separate detailed analysis which remains out of the scope of this paper.

Acknowledgement

The work of R. Lazarov has been partially supported by the grant NSF-DMS #1620318. The work of S. Harizanov, Y. Vutov and P. Marinov has been partially supported by the Bulgarian National Fund under grants M 02/3 and I-02/20, respectively.

References

[1] O. G. Bakunin. *Turbulence and diffusion: scaling versus equations*. Springer Science & Business Media, 2008.
[2] P. W. Bates. On some nonlocal evolution equations arising in materials science. *Nonlinear dynamics and evolution equations*, 48:13–52, 2006.
[3] A. Bonito and J. Pasciak. Numerical approximation of fractional powers of elliptic operators. *Mathematics of Computation*, 84(295):2083–2110, 2015.
[4] L. Chen, R. Nochetto, O. Enrique, and A. J. Salgado. Multilevel methods for nonuniformly elliptic operators and fractional diffusion. *Mathematics of Computation*, 85:2583–2607, 2016.
[5] E. W. Cheney and M. J. D. Powell. The differential correction algorithm for generalized rational functions. *Constructive Approximation*, 3(1):249–256, 1987.
[6] W. J. Cody, G. Meinardus, and R. S. Varga. Chebyshev rational approximation to e^{-x} in $[0, +\infty)$ and applications to heat-conducttion problems. *Journal of Approximation Theory*, 2:50–65, 1969.
[7] V. Druskin and L. Knizhnerman. Extended Krylov subspaces: approximation of the matrix square root and related functions. *SIAM Journal on Matrix Analysis and Applications*, 19(3):755–771, 1998.
[8] C. B. Dunham. Difficulties in rational Chebyshev approximation. In *Conference on Constructive Theory of Functions, Varna, Bulgaria*, pages 319–327, 1984.
[9] I. Gavrilyuk, W. Hackbusch, and B. Khoromskij. Hierarchical tensor-product approximation to the inverse and related operators for high dimensional elliptic problems. *Computing*, 74(2):131–157, 2005.
[10] G. Gilboa and S. Osher. Nonlocal operators with applications to image processing. *Multiscale Modeling & Simulation*, 7(3):1005–1028, 2008.
[11] S. Harizanov, S. Margenov, P. Marinov, and Y. Vutov. Volume constrained 2-phase segmentation method utilizing a linear system solver based on the best uniform polynomial approximation of $x^{-1/2}$. *Journal of Computational and Applied Mathematics*, 310:115–128, 2017.
[12] V. E. Henson and U. M. Yang. Boomeramg: A parallel algebraic multigrid solver and preconditioner. *Applied Numerical Mathematics*, 41(1):155 – 177, 2002.
[13] N. J. Higham. Stable iterations for the matrix square root. *Numerical Algorithms*, 15(2):227–242, 1997.
[14] M. Ilić, I. W. Turner, and V. Anh. A numerical solution using an adaptively preconditioned Lanczos method for a class of linear systems related with the fractional Poisson equation. *International Journal of Stochastic Analysis*, 2008, 2009.
[15] C. Kenney and A. J. Laub. Rational iterative methods for the matrix sign function. *SIAM J. Matrix Anal. Appl.*, 12(2):273–291, Mar. 1991.
[16] A. Kilbas, H. Srivastava, and J. Trujillo. *Theory and Applications of Fractional Differential Equations*. Elsevier, Amsterdam, 2006.
[17] P. G. Marinov and A. S. Andreev. A modified Remez algorithm for approximate determination of the rational function of the best approximation in Hausdorff metric. *Comptes rendus de l'Academie bulgare des Scieces*, 40(3):13–16, 1987.
[18] B. McCay and M. Narasimhan. Theory of nonlocal electromagnetic fluids. *Archives of Mechanics*, 33(3):365–384, 1981.
[19] R. Metzler, J.-H. Jeon, A. G. Cherstvy, and E. Barkai. Anomalous diffusion models and their properties: non-stationarity, non-ergodicity, and ageing at the centenary of single particle tracking. *Physical Chemistry Chemical Physics*, 16(44):24128–24164, 2014.
[20] S. Nepomnyaschikh. Mesh theorems on traces, normalizations of function traces and their inversion. *Sov. J. Numer. Anal. Math. Modelling*, 6(3):223–242, 1991.
[21] S. A. Silling. Reformulation of elasticity theory for discontinuities and long-range forces. *Journal of the Mechanics and Physics of Solids*, 48(1):175–209, 2000.
[22] P. N. Vabishchevich. Numerically solving an equation for fractional powers of elliptic operators. *Journal of Computational Physics*, 282:289–302, 2015.
[23] J. Xu and L. Zikatanov. The method of alternating projections and the method of subspace corrections in Hilbert space. *Journal of the American Mathematical Society*, 15(3):573–597, 2002.
[24] G. M. Zaslavsky. Chaos, fractional kinetics, and anomalous transport. *Physics Reports*, 371(6):461–580, 2002.

6. Appendix

Institute of Information and Communication Technologies, Bulgarian Academy of Sciences, Acad. G. Bonchev, bl. 25A, 1113 Sofia, Bulgaria (sharizanov@parallel.bas.bg)

TABLE 9. The coefficients in the representation (16) of 1-BURA $P_7^*(t)/Q_7^*(t)$ of $t^{1-\alpha}$ on $[0,1]$

j	$\alpha = 0.25$		$\alpha = 0.5$		$\alpha = 0.75$	
	c_j	d_j	c_j	d_j	c_j	d_j
0	3.25659E-06	0.00000E+00	4.60366E-05	0.00000E+00	7.85127E-04	0.00000E+00
1	1.44761E-04	-8.74568E-06	9.55918E-04	-3.58368E-07	6.54730E-03	-2.21777E-10
2	1.08271E-03	-2.17427E-04	4.65253E-03	-1.93872E-05	1.81424E-02	-7.80406E-08
3	5.25468E-03	-2.38575E-03	1.63200E-02	-3.71546E-04	4.17928E-02	-5.55397E-06
4	2.05418E-02	-1.77397E-02	4.80082E-02	-4.34363E-03	8.61599E-02	-1.88388E-04
5	7.43766E-02	-1.07563E-01	1.28889E-01	-3.80180E-02	1.65247E-01	-4.07531E-03
6	3.36848E-01	-6.71407E-01	3.73943E-01	-3.00901E-01	3.11865E-01	-6.65806E-02
7	1.16449E+01	-1.55256E+01	2.94945E+00	-4.68768E+00	8.94453E-01	-1.30039E+00

TABLE 10. The coefficients in the representation (16) of 2-BURA $P_5^*(t)/Q_4^*(t)$ of $t^{2-\alpha}$ on $[0,1]$

j	$\alpha = 0.25$		$\alpha = 0.5$		$\alpha = 0.75$	
	c_j	d_j	c_j	d_j	c_j	d_j
0,1	3.37593E-03	0.00000E+00	2.34402E-02	0.00000E+00	1.42137E-01	0.00000E+00
0,2	-6.2333E-07	0.00000E+00	-2.0349E-06	0.00000E+00	-3.8415E-06	0.00000E+00
1	2.40583E-02	-1.47434E-02	7.84172E-02	-8.08787E-03	1.69113E-01	-3.82073E-03
2	8.72123E-02	-1.22415E-01	1.75667E-01	-7.81739E-02	2.20935E-01	-4.55009E-02
3	3.80068E-01	-7.92754E-01	4.54976E-01	-5.27883E-01	3.41427E-01	-3.37721E-01
4	1.30317E+01	-1.80742E+01	3.58723E+00	-7.18890E+00	1.04996E+00	-3.71162E+00

TABLE 11. The coefficients in the representation (16) of 2-BURA $P_7^*(t)/Q_6^*(t)$ of $t^{2-\alpha}$ on $[0,1]$

j	$\alpha = 0.25$		$\alpha = 0.5$		$\alpha = 0.75$	
	c_j	d_j	c_j	d_j	c_j	d_j
0,1	7.38825E-04	0.00000E+00	7.91901E-03	0.00000E+00	7.87824E-02	0.00000E+00
0,2	-1.8043E-08	0.00000E+00	-7.8577E-08	0.00000E+00	-2.0108E-07	0.00000E+00
1	5.14919E-03	-1.91822E-03	2.62088E-02	-9.16055E-04	9.33258E-02	-3.59264E-04
2	1.66782E-02	-1.48538E-02	5.50057E-02	-8.44288E-03	1.17911E-01	-4.15349E-03
3	4.59429E-02	-7.22366E-02	1.06623E-01	-4.61173E-02	1.53620E-01	-2.65144E-02
4	1.29584E-01	-2.99678E-01	2.11649E-01	-2.05570E-01	2.09664E-01	-1.31566E-0
5	5.25079E-01	-1.41237E+00	5.39001E-01	-9.66103E-01	3.42629E-01	-6.42203E-01
6	1.81241E+01	-2.83519E+01	4.40913E+00	-1.12571E+01	1.13935E+00	-5.82558E+00

DEPTARTMENT OF MATHEMATICS, TEXAS A&M UNIVERSITY, COLLEGE STATION, TX 77843-3368, USA (LAZAROV@MATH.TAMU.EDU) AND INSTITUTE OF MATHEMATICS AND INFORMATICS, BULGARIAN ACADEMY OF SCIENCES, ACAD. G. BONCHEV, BL. 8, 1113 SOFIA, BULGARIA

INSTITUTE OF INFORMATION AND COMMUNICATION TECHNOLOGIES, BULGARIAN ACADEMY OF SCIENCES, ACAD. G. BONCHEV, BL. 25A, 1113 SOFIA, BULGARIA (PENCHO@PARALLEL.BAS.BG)

INSTITUTE OF INFORMATION AND COMMUNICATION TECHNOLOGIES, BULGARIAN ACADEMY OF SCIENCES, ACAD. G. BONCHEV, BL. 25A, 1113 SOFIA, BULGARIA (MARGENOV@PARALLEL.BAS.BG)

INSTITUTE OF INFORMATION AND COMMUNICATION TECHNOLOGIES, BULGARIAN ACADEMY OF SCIENCES, ACAD. G. BONCHEV, BL. 25A, 1113 SOFIA, BULGARIA (YAVOR@PARALLEL.BAS.BG)

TABLE 12. Numerical error ε in (9) for $(m,k)=(7,7)$ and $\beta=1$. For each α the left column shows the results for $\mathbf{f}$ consisting of eigenvectors, while the right column is the error for $\mathbf{f}$ taken as 1000 random eigenvector combinations. In each box averaged error (top) and the maximal error (bottom) are reported.

h^{-1}	$\alpha=0.25$		$\alpha=0.5$		$\alpha=0.75$	
	$E_\alpha(7,7;1)=$**3.2566**E-06		$E_\alpha(7,7;1)=$**4.6037**E-05		$E_\alpha(7,7;1)=$**7.8966**E-04	
	$\{\mathbf{\Psi}_i\}_{i=1}^N$	rand1000	$\{\mathbf{\Psi}_i\}_{i=1}^N$	rand1000	$\{\mathbf{\Psi}_i\}_{i=1}^N$	rand1000
8	1.9565E-06	1.7915E-06	2.8431E-05	2.7493E-05	5.6995E-04	6.9670E-04
	3.2061E-06	2.9876E-06	4.6024E-05	4.5356E-05	7.6989E-04	7.6437E-04
16	2.0032E-06	2.4354E-06	2.6759E-05	2.3804E-05	5.2532E-04	6.5826E-04
	3.1948E-06	2.9711E-06	4.5812E-05	3.7222E-05	7.8518E-04	7.0151E-04
32	2.1362E-06	2.7011E-06	2.9166E-05	3.3229E-05	5.0559E-04	5.9927E-04
	3.2522E-06	2.9153E-06	4.5720E-05	3.7850E-05	7.8286E-04	6.4667E-04
64	2.0616E-06	1.9800E-06	2.9487E-05	3.9642E-05	4.9911E-04	4.8683E-04
	3.2564E-06	2.8259E-06	4.6035E-05	4.3436E-05	7.8744E-04	6.3295E-04
128	2.0567E-06	1.5541E-06	2.9505E-05	4.0691E-05	4.9672E-04	3.5982E-04
	3.2565E-06	2.6089E-06	4.6033E-05	4.4048E-05	7.8922E-04	6.7316E-04
256	2.0675E-06	1.8786E-06	2.9370E-05	3.8431E-05	4.9953E-04	4.4143E-04
	3.2566E-06	2.6313E-06	4.6029E-05	4.3061E-05	7.8959E-04	7.0087E-04
512	2.0734E-06	2.6468E-06	2.9312E-05	3.0132E-05	5.0116E-04	6.3817E-04
	3.2566E-06	3.0750E-06	4.6036E-05	3.9441E-05	7.8965E-04	7.4051E-04
1024	2.0736E-06	2.3078E-06	2.9288E-05	2.3497E-05	5.0152E-04	6.3749E-04
	3.2566E-06	2.9537E-06	4.6037E-05	3.7366E-05	7.8965E-04	7.1731E-04

TABLE 13. Numerical error ε in (9) for $(m,k)=(7,6)$ and $\beta=2$. For each α the left column shows the results for $\mathbf{f}$ consisting of eigenvectors, while the right column is the error for $\mathbf{f}$ taken as 1000 random eigenvector combinations. In each box averaged error (top) and the maximal error (bottom) are reported.

h^{-1}	$\alpha=0.25$		$\alpha=0.5$		$\alpha=0.75$	
	$E_\alpha(7,6;2)=$**1.8043**E-08		$E_\alpha(7,6;2)=$**7.8577**E-08		$E_\alpha(7,6;2)=$**2.0108**E-07	
	$\{\mathbf{\Psi}_i\}_{i=1}^N$	rand1000	$\{\mathbf{\Psi}_i\}_{i=1}^N$	rand1000	$\{\mathbf{\Psi}_i\}_{i=1}^N$	rand1000
8	1.0632E-08	1.0631E-08	5.9400E-08	6.0261E-08	1.0966E-07	1.0468E-07
	1.5547E-08	1.2642E-08	7.8416E-08	6.9105E-08	2.01E00-07	1.5912E-07
16	9.5732E-09	1.3119E-08	5.4368E-08	5.3487E-08	1.1609E-07	1.7237E-07
	1.7828E-08	1.3955E-08	7.7768E-08	7.6782E-08	2.0032E-07	1.8421E-07
32	1.1235E-08	3.6625E-09	5.1080E-08	7.5291E-08	1.2520E-07	6.2571E-08
	1.8049E-08	1.5797E-08	7.8585E-08	7.8456E-08	2.0100E-07	1.9484E-07
64	1.1198E-08	3.2757E-09	5.1082E-08	7.7033E-08	1.2412E-07	2.8021E-08
	1.8040E-08	1.0433E-08	7.8644E-08	7.8491E-08	2.0090E-07	9.7132E-08
128	1.1468E-08	1.6223E-08	5.0090E-08	6.7111E-08	1.2665E-07	5.8966E-08
	1.8066E-08	1.7177E-08	7.8573E-08	7.7379E-08	2.0110E-07	1.4951E-07
256	1.1446E-08	3.8759E-09	4.9977E-08	4.4867E-08	1.2795E-07	1.8929E-07
	1.8062E-08	1.7213E-08	7.8638E-08	6.9319E-08	2.0111E-07	2.0039E-07
512	1.1473E-08	1.1522E-08	4.9994E-08	3.1754E-08	1.2783E-07	6.5736E-08
	1.8065E-08	1.2699E-08	7.8647E-08	7.0909E-08	2.0111E-07	1.9958E-07

TABLE 14. Numerical error ε in (9) for the multi-step case $(m,k)=(5,5)$ and $\beta=1$. For each setup the left column shows the results for $\mathbf{f}$ consisting of eigenvectors, while the right column is the error for $\mathbf{f}$ taken as 1000 random eigenvector combinations. In each box averaged error (top) and the maximal error (bottom) are reported.

h^{-1}	$\alpha=0.5$		$\alpha=0.75$		$\alpha=0.75$	
	$\mathbf{u}_r=\mathcal{A}^{-0.25}\left(\mathcal{A}^{-0.25}\mathbf{f}\right)$		$\mathbf{u}_r=\mathcal{A}^{-0.25}\left(\mathcal{A}^{-0.25}\left(\mathcal{A}^{-0.25}\mathbf{f}\right)\right)$		$\mathbf{u}_r=\mathcal{A}^{-0.25}\left(\mathcal{A}^{-0.50}\mathbf{f}\right)$	
	$\{\mathbf{\Psi}_i)\}_{i=1}^N$	rand1000	$\{\mathbf{\Psi}_i)\}_{i=1}^N$	rand1000	$\{\mathbf{\Psi}_i)\}_{i=1}^N$	rand1000
16	4.1065E-05	4.1827E-05	8.7666E-05	1.2954E-04	1.9972E-04	1.7173E-04
	9.4745E-05	7.2813E-05	2.3891E-04	2.2187E-04	3.9098E-04	3.3170E-04
32	4.7118E-05	5.1558E-05	1.0939E-04	2.0585E-04	2.1337E-04	2.3155E-04
	1.2093E-04	1.0361E-04	4.8074E-04	3.9256E-04	5.0294E-04	4.1310E-04
64	5.1447E-05	1.0267E-04	1.4007E-04	7.7816E-04	2.3385E-04	4.5311E-04
	2.0432E-04	1.5404E-04	1.1396E-03	9.9375E-04	5.6349E-04	5.4832E-04
128	5.7422E-05	3.2390E-04	2.0400E-04	4.1774E-03	2.3648E-04	4.0115E-04
	4.5572E-04	4.3974E-04	6.2524E-03	6.0171E-03	5.9066E-04	5.4683E-04
256	5.9104E-05	4.3670E-04	2.3325E-04	7.4754E-03	2.3848E-04	7.7769E-04
	5.3831E-04	5.2302E-04	1.0097E-02	9.7472E-03	1.0680E-03	1.0328E-03
512	5.9310E-05	5.9445E-04	2.4906E-04	1.3916E-02	2.4811E-04	3.8679E-03
	7.7978E-04	7.5465E-04	1.9729E-02	1.9016E-02	5.8996E-03	5.6791E-03
1024	5.9021E-05	4.1906E-04	2.4148E-04	9.6104E-03	2.5064E-04	5.3558E-03
	8.0305E-04	7.2124E-04	1.9733E-02	1.7263E-02	6.8130E-03	6.5918E-03

TABLE 15. Numerical error ε in (9) for the multi-step case $(m,k)=(7,7)$ and $\beta=1$. For each setup the left column shows the results for $\mathbf{f}$ consisting of eigenvectors, while the right column is the error for $\mathbf{f}$ taken as 1000 random eigenvector combinations. In each box averaged error (top) and the maximal error (bottom) are reported.

h^{-1}	$\alpha=0.5$		$\alpha=0.75$		$\alpha=0.75$	
	$\mathbf{u}_r=\mathcal{A}^{-0.25}\left(\mathcal{A}^{-0.25}\mathbf{f}\right)$		$\mathbf{u}_r=\mathcal{A}^{-0.25}\left(\mathcal{A}^{-0.25}\left(\mathcal{A}^{-0.25}\mathbf{f}\right)\right)$		$\mathbf{u}_r=\mathcal{A}^{-0.25}\left(\mathcal{A}^{-0.50}\mathbf{f}\right)$	
	$\{\mathbf{\Psi}_i)\}_{i=1}^N$	rand1000	$\{\mathbf{\Psi}_i)\}_{i=1}^N$	rand1000	$\{\mathbf{\Psi}_i)\}_{i=1}^N$	rand1000
8	5.0192E-06	5.1628E-06	1.0010E-05	1.1877E-05	3.6246E-05	4.0301E-05
	9.8128E-06	9.6002E-06	2.5169E-05	2.4547E-05	7.0309E-05	6.8761E-05
16	5.8605E-06	1.4026E-05	1.5501E-05	6.6467E-05	3.4149E-05	3.7829E-05
	1.9834E-05	1.9260E-05	9.7937E-05	9.4949E-05	6.6285E-05	5.2376E-05
32	6.7145E-06	2.0145E-05	2.0351E-05	1.2619E-04	3.9973E-05	8.4991E-05
	2.5714E-05	2.5005E-05	1.7685E-04	1.7140E-04	1.1430E-04	1.1152E-04
64	6.3275E-06	1.8390E-05	1.9405E-05	1.4991E-04	4.3354E-05	1.6584E-04
	2.6754E-05	2.3775E-05	1.8260E-04	1.7894E-04	2.2211E-04	2.1671E-04
128	6.3162E-06	1.7655E-05	1.9982E-05	1.9293E-04	4.5322E-05	2.5209E-04
	2.7195E-05	2.1459E-05	2.3671E-04	2.3119E-04	3.2535E-04	3.1700E-04
256	6.5595E-06	3.5085E-05	2.4035E-05	5.9986E-04	4.5112E-05	2.3879E-04
	4.5202E-05	4.4046E-05	8.6567E-04	8.3841E-04	3.1927E-04	2.9358E-04
512	6.7797E-06	8.1866E-05	2.9931E-05	2.1139E-03	4.6091E-05	4.4815E-04
	1.1361E-04	1.0915E-04	3.1081E-03	2.9789E-03	5.7114E-04	5.5602E-04
1024	6.8055E-06	9.0098E-05	3.1472E-05	3.0128E-03	4.7830E-05	1.1992E-03
	1.1366E-04	1.0352E-04	3.9165E-03	3.8048E-03	1.6865E-03	1.6425E-03

TABLE 16. Numerical ℓ^2-error ε for $h^{-1} = 2^n$ based on (33) for $\mathbf{f}$ reconstruction with $(m, k) = (5, 5)$ and $\beta = 1$. For each setup the left column shows the results for $\mathbf{f}$ consisting of eigenvectors, while in the middle and right columns are the errors for $\mathbf{f}$ taken as 1000 random eigenvector combinations. In each box averaged error (top) and the maximal error (bottom) are reported.

h^{-1}	$\mathcal{A}(\mathcal{A}^{-0.25}(\mathcal{A}^{-0.75}\mathbf{f}))$			$\mathcal{A}(\mathcal{A}^{-0.5}(\mathcal{A}^{-0.5}\mathbf{f}))$		
	$E_{0.75} + E_{0.25} - E_{0.75}E_{0.25} =$**2.7448**E-03			$2E_{0.5} - E_{0.5}^2 =$**5.3784**E-04		
	$\{\mathbf{\Psi}_i)\}_{i=1}^N$	rand1000	rand1000	$\{\mathbf{\Psi}_i)\}_{i=1}^N$	rand1000	rand1000
16	4.7354E-04	7.5219E-05	7.5147E-05	1.0598E-04	8.7507E-06	8.6706E-06
	2.4855E-03	8.1696E-05	8.2122E-05	4.8149E-04	1.3993E-05	1.5610E-05
32	4.7350E-04	2.4231E-05	2.4240E-05	1.0689E-04	4.0082E-06	3.9951E-06
	2.6751E-03	2.5452E-05	2.5517E-05	5.1127E-04	6.8881E-06	6.7313E-06
64	4.7775E-04	3.4729E-06	3.4744E-06	1.0850E-04	6.9353E-06	6.9349E-06
	2.7268E-03	4.0236E-06	3.9443E-06	5.3095E-04	7.3211E-06	7.2493E-06
128	4.7955E-04	6.0366E-07	6.0448E-07	1.0878E-04	6.2346E-06	6.2351E-06
	2.7402E-03	8.7980E-07	9.4323E-07	5.3609E-04	6.2777E-06	6.2911E-06
256	4.8034E-04	5.7357E-07	5.7343E-07	1.0891E-04	2.5050E-06	2.5049E-06
	2.7437E-03	5.8741E-07	5.8982E-07	5.3740E-04	2.5149E-06	2.5144E-06
512	4.8074E-04	1.2493E-06	1.2493E-06	1.0895E-04	6.7062E-07	6.7059E-07
	2.7445E-03	1.2496E-06	1.2496E-06	5.3773E-04	6.7463E-07	6.7458E-07
1024	4.8094E-04	2.0673E-07	2.0677E-07	1.0898E-04	6.9352E-07	6.9357E-07
	2.7447E-03	2.0885E-07	2.0924E-07	5.3781E-04	6.9625E-07	6.9637E-07
2048	4.8104E-04	4.1620E-07	4.1620E-07	1.0899E-04	2.8010E-07	2.8010E-07
	2.7448E-03	4.1646E-07	4.1649E-07	5.3783E-04	2.8034E-07	2.8027E-07
4096	4.8109E-04	5.3275E-07	5.3275E-07	1.0900E-04	3.6167E-08	3.6185E-08
	2.7448E-03	5.3281E-07	5.3282E-07	5.3784E-04	3.7534E-08	3.7333E-08

TABLE 17. Numerical ℓ^2-error ε for $h^{-1} = 2^n$ based on (33) for $\mathbf{f}$ reconstruction with $(m, k) = (7, 7)$ and $\beta = 1$. For each setup the left column shows the results for $\mathbf{f}$ consisting of eigenvectors, while in the middle and right columns are the errors for $\mathbf{f}$ taken as 1000 random eigenvector combinations. In each box averaged error (top) and the maximal error (bottom) are reported.

h^{-1}	$\mathcal{A}(\mathcal{A}^{-0.25}(\mathcal{A}^{-0.75}\mathbf{f}))$			$\mathcal{A}(\mathcal{A}^{-0.5}(\mathcal{A}^{-0.5}\mathbf{f}))$		
	$E_{0.75} + E_{0.25} - E_{0.75}E_{0.25} =$**7.9291**E-04			$2E_{0.5} - E_{0.5}^2 =$**9.2071**E-05		
	$\{\mathbf{\Psi}_i)\}_{i=1}^N$	rand1000	rand1000	$\{\mathbf{\Psi}_i)\}_{i=1}^N$	rand1000	rand1000
16	2.7428E-04	1.9574E-05	1.9581E-05	3.6147E-05	3.6776E-06	3.6796E-06
	6.9284E-04	2.2126E-05	2.1900E-05	8.3254E-05	3.9151E-06	3.9819E-06
32	2.7502E-04	5.8770E-06	5.8751E-06	3.7098E-05	3.6259E-06	3.6258E-06
	7.6589E-04	6.5626E-06	6.3826E-06	8.5885E-05	3.7467E-06	3.7298E-06
64	2.7683E-04	1.3628E-06	1.3604E-06	3.7178E-05	2.1428E-06	2.1423E-06
	7.8591E-04	1.5488E-06	1.5196E-06	9.0463E-05	2.1745E-06	2.1682E-06
128	2.7801E-04	2.2851E-07	2.3003E-07	3.7255E-05	1.0873E-06	1.0873E-06
	7.9113E-04	3.2669E-07	3.2927E-07	9.1662E-05	1.0939E-06	1.0921E-06
256	2.7853E-04	3.4135E-07	3.4141E-07	3.7286E-05	4.9867E-07	4.9869E-07
	7.9246E-04	3.5032E-07	3.5252E-07	9.1968E-05	4.9986E-07	5.0030E-07
512	2.7875E-04	3.0366E-07	3.0365E-07	3.7300E-05	1.4905E-07	1.4905E-07
	7.9280E-04	3.0476E-07	3.0452E-07	9.2045E-05	1.4975E-07	1.4971E-07
1024	2.7886E-04	1.2014E-07	1.2014E-07	3.7307E-05	4.3477E-08	4.3476E-08
	7.9288E-04	1.2029E-07	1.2030E-07	9.2065E-05	4.4327E-08	4.4182E-08
2048	2.7892E-04	7.9001E-08	7.9001E-08	3.7312E-05	7.2197E-08	7.2198E-08
	7.9290E-04	7.9031E-08	7.9026E-08	9.2069E-05	7.2315E-08	7.2295E-08
4096	2.7895E-04	5.2692E-09	5.2567E-09	3.7314E-05	1.1877E-08	1.1875E-08
	7.9291E-04	5.8000E-09	5.6822E-09	9.2071E-05	1.1928E-08	1.1916E-08